Tectonics

RESEARCH ARTICLE
10.1029/2025TC009110

Crustal Thickness and Elevation of the North American Cordillera From the Late Cretaceous to the Early Miocene

L. C. Basler[1], B. Carrapa[1], P. Kapp[1], and M. N. Ducea[1,2]

[1]Department of Geosciences, University of Arizona, Tucson, AZ, USA, [2]Faculty of Geology and Geophysics, University of Bucharest, Bucharest, Romania

Key Points:

- Geochemical proxies indicate thick crust (55 km) and high paleoelevations (3.6 km) extended >1,500 km along-strike in the Cordillera
- An orogenic highland was maintained until the Early Miocene (ca. 20 Ma) in the central and southern segments of the Cordillera (30–42°N)
- Metamorphic core complexes exhumed in regions of previously thickened crust

Supporting Information:

Supporting Information may be found in the online version of this article.

Correspondence to:

L. C. Basler,
lukebasler@arizona.edu

Citation:

Basler, L. C., Carrapa, B., Kapp, P., & Ducea, M. N. (2026). Crustal thickness and elevation of the North American Cordillera from the Late Cretaceous to the Early Miocene. *Tectonics*, *45*, e2025TC009110. https://doi.org/10.1029/2025TC009110

Received 21 JUL 2025
Accepted 4 DEC 2025

Abstract Cordilleran-type orogenic systems are characterized by high elevation regions that form in the hinterland of long-lived convergent continental arcs. Despite their global tectonic and climatic significance, reconstructing past surface elevations and crustal thicknesses of these highlands has proved difficult, necessitating new methodological approaches. Here we apply geochemical proxies to expand the spatial and temporal resolution of paleoelevation and paleocrustal thickness estimates in the North American Cordillera (30–49°N). We compiled arc geochemical data ($n = 11{,}865$) from the Late Cretaceous to the Early Miocene (95–17 Ma). Using new chemical "mohometers," we construct maps of crustal thickness and elevation at 1 Ma intervals. We also generate time series for the southern, central, and northern segments of the orogen, calculate crustal thickness at the onset of metamorphic core complex exhumation, and compare our results to previous stable isotope paleoaltimetry studies. Results indicate that a Paleogene highland was continuous for 1,500 km along-strike of the North American Cordillera, consistent with previous stable isotope, structural, and geochemical data. This region was characterized by crustal thicknesses between 50 and 60 km (mean = 54.8 km) and paleoelevations between 3 and 4 km (mean = 3.6 km). In the central and southern segments (Nevada and western Arizona) crust at least 50 km thick was present until the Early Miocene, which suggests that thickened crust was maintained for a protracted interval following Cretaceous shortening. These results indicate that most crustal thinning was contemporaneous with a change in plate boundary conditions along the western North American margin.

Plain Language Summary In western North America, many modern mountains represent the extended, collapsed remnants of a former high-elevation region. The past elevation and areal extent of this region remain controversial, which limits our understanding of the processes that construct high-elevation, plateau-like mountains and contribute to their subsequent extensional demise. We apply a recently developed tool to reconstruct the elevation and crustal thickness of western North America (from northern Montana and Idaho through southern Arizona) between 17 and 95 million years ago. The tool uses the geochemistry of igneous rocks to reconstruct past elevation and crustal thickness during their eruption or emplacement in the crust. Our results suggest that a broad, high-elevation region with an average elevation of about 3.6 km extended across much of western North America, analogous to segments of the modern Central Andes in South America. This highland persisted until fairly recently (~17 million years ago), suggesting that widespread extension and collapse of this high elevation region was linked to a transition in the type of plate boundary on the western margin of the North American plate.

1. Introduction

Cordilleran-type orogenic systems host some of the highest elevations and thickest crust on Earth (e.g., Beck et al., 1996; Garzione et al., 2017). Crustal thickening and surface uplift in Cordilleran orogens are the product of long-duration shortening in the retro-arc fold-and-thrust belt, which underthrusts lithosphere trench-ward to construct a thickened, crustal welt in the hinterland (DeCelles et al., 2009; Long, 2023). As a result of high surface elevations and thick crust, past Cordilleran-type orogens exerted an important control on global and regional climate, biological evolution, and basin formation (DeCelles & Giles, 1996; Garzione et al., 2008; Kent-Corson et al., 2013; C.-T. A. Lee et al., 2015; Smiley et al., 2024).

The Mesozoic–Cenozoic North American Cordillera was an archetypal Cordilleran-type orogenic system that persisted from the Late Jurassic until extensional collapse in the mid-to-late Cenozoic (DeCelles, 2004; Dickinson, 2004; Ducea et al., 2015). From the trench inboard, the orogen featured an accretionary wedge, forearc

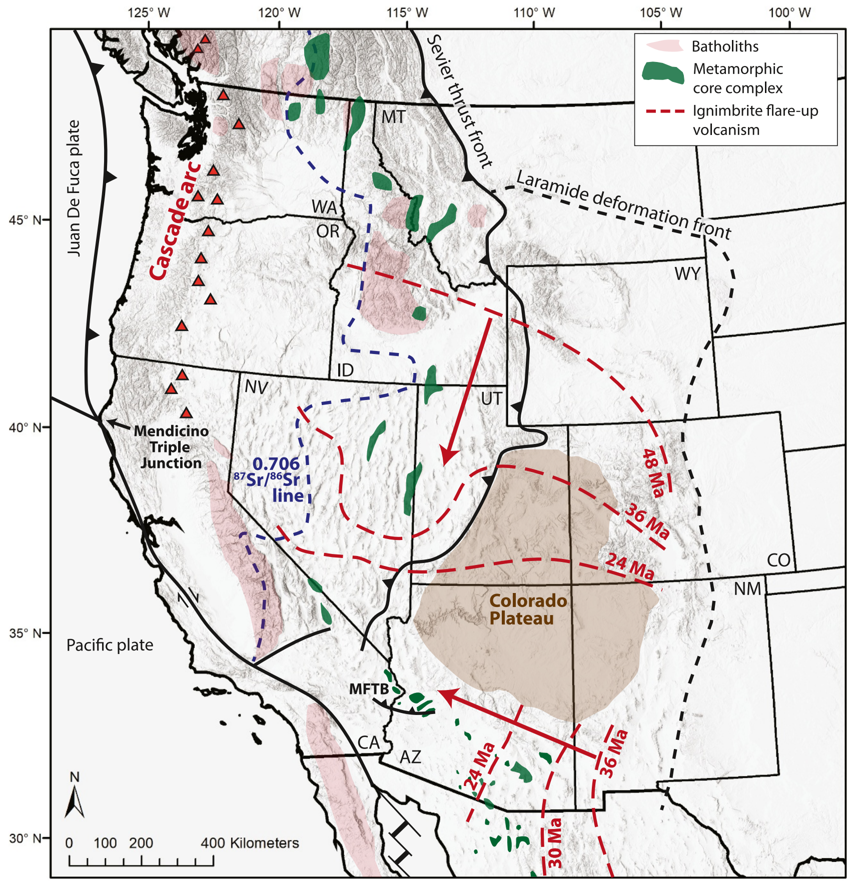

Figure 1. Simplified tectonic map of the western North American Cordillera. The dashed red lines indicate the migration of ignimbrite flare-up volcanism during foundering of the Farallon slab, modified from Best et al. (2016) and Humphreys (1995). MFTB—Maria fold-and-thrust belt.

basin, magmatic arc, hinterland orogenic highland, retro-arc fold-and-thrust belt, and foreland basin. First-order changes in the style and location of upper plate deformation in the hinterland are generally interpreted to correspond to changes in the dip of the subducting Farallon slab (Coney & Reynolds, 1977; Copeland et al., 2017). Normal-dipping subduction (~20–40° at depths of <125 km; Schellart & Strak, 2021) in the Early to mid Cretaceous produced thin-skinned, east-propagating deformation in the Sevier retro-arc fold-and-thrust belt, while slab flattening ca. 80–90 Ma corresponded to a shift toward higher-angle, basement-involved, Laramide-style deformation east of the frontal Sevier belt (Humphreys, 2009; Jepson et al., 2025; Jones et al., 2011; Weil & Yonkee, 2023; Yonkee & Weil, 2015). Slab flattening extinguished arc magmatism at coastal batholiths and caused the discontinuous inboard migration of the arc, along with a general dissipation in the fluxes of arc magmatism. Following accretion of the Siletzia oceanic plateau ca. 53 Ma, rollback or foundering of the Farallon flat slab corresponded to exhumation along a belt of metamorphic core complexes (MCCs) and high-flux volcanism during the "ignimbrite flare-up" (Armstrong & Ward, 1991; Coney & Harms, 1984; Dickinson & Snyder, 1979; Glazner, 2022; Lipman et al., 1972; Schmandt & Humphreys, 2011). Syn-rollback volcanism was diachronous across two trends that met in southern Nevada (~36°N) at ca. 17 Ma: a south or southwest-younging trend beginning in Idaho and Montana and a northwest-younging trend across Arizona (Figure 1; Humphreys, 1995; McQuarrie & Oskin, 2010). The ca. 28–30 Ma onset of the transition to a transform or transtensional margin resulted from subduction of an oceanic spreading ridge, followed by the onset of Basin-and-Range-style extension at ca. 17 Ma (e.g., Atwater, 1970; Atwater & Stock, 1998; Colgan et al., 2006; Coney, 1987; Dickinson, 2002; Zuza, Jepson, & Cao, 2024).

A variety of geochemical, structural, isotopic, and paleobiologic data sets have been used to reconstruct crustal thickness and elevation of the hinterland of the North American Cordillera (e.g., Chamberlain et al., 2021; Licht

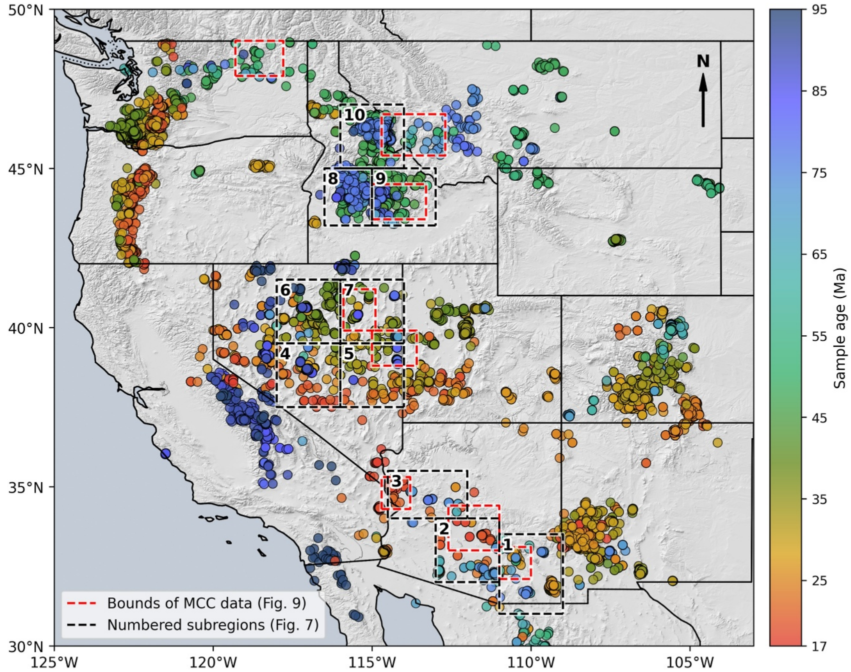

Figure 2. Map of whole-rock geochemical samples used to calculate crustal thickness and elevation. Sample color corresponds to age. Black and red boxes indicate the bounds of data used in chemical mohometry calculations in Figures 7 and 9, respectively. MCC—Metamorphic Core Complex.

et al., 2017; Long, 2023; Wolfe et al., 1998). Broadly, these studies indicate the presence of relatively thick crust and high elevations spanning from southern Canada to northern Mexico by the Late Cretaceous or early Paleogene. Despite general agreement about the existence of this high-elevation feature across western North America, uncertainties persist about the spatial footprint, maximum elevation and crustal thickness, and relief of this highland. For instance, some geochemical reconstructions of crustal thickness favor thick Late Cretaceous and early Cenozoic crust (70+ km) comparable to the modern central Andes in the Nevada segment of the orogen (Best et al., 2009, 2016), while other studies prefer more modest crustal thicknesses of 45–50 km (e.g., Konstantinou, 2022; Lund Snee & Miller, 2022). Resolving these discrepancies is essential to both understanding the mechanisms governing changes in crustal thickness and assessing the potential climatic, erosional, and geodynamic implications of thickened crust and high elevations (DeCelles & Carrapa, 2023; Feng et al., 2013; Fricke et al., 2010; Molnar & Lyon-Caen, 1988; Painter et al., 2014; Sewall & Sloan, 2006).

The mechanisms responsible for extensional thinning in the central and southern segments (~30–42°N) of the orogenic hinterland also remain unclear (Axen et al., 1993; Gans, 1987; Sonder & Jones, 1999; Wernicke, 1992; Wernicke et al., 1987). Modern crustal thicknesses in this region are ~30 ± 5 km (Laske et al., 2013; Figure 3, inset map). If crustal thicknesses were ~55 km during the Late Cretaceous (e.g., J. B. Chapman et al., 2015), ~20–30 km of subsequent crustal thinning is required. Proposed models of thinning can be broadly classified into two endmembers, each of which emphasizes distinct mechanisms of orogenic collapse: (a) The first model argues that most crustal thinning occurred in the Miocene, after subduction of a spreading ridge resulted in a transition to a dextral transform margin during the north and south-directed migrations of the Mendocino and Rivera triple junctions, respectively (Best & Christiansen, 1991; Best et al., 2009, 2016; Cassel et al., 2014, 2018; Colgan & Henry, 2009; Colgan et al., 2010; Henry et al., 2011; Lund Snee & Miller, 2022; E. L. Miller et al., 1999). This model implies that crustal thinning was linked to a change in boundary conditions during this plate margin reorganization and suggests that high elevations and thickened crust largely persisted into the Early Miocene, at least 30 Ma after the cessation of shortening in most of the Cordillera. (b) A second model suggests that crustal thinning initiated earlier, during rollback of the Farallon flat slab and coeval ignimbrite flare-up volcanism. This model argues that crustal thinning was partitioned into distinct phases over a more protracted interval, and implicates thermal weakening, removal of the Farallon slab, or the syn-rollback acquisition of lithospheric buoyancy as a driver of thinning (Armstrong & Ward, 1991; Gans et al., 1989; Jones et al., 1998; Sonder & Jones, 1999).

Each of these models make distinct predictions about the pre-Basin-and-Range evolution of crustal thickness in the Cordillera: The former predicts limited changes in crustal thickness until Basin-and-Range extension (ca. 17 Ma) while the latter predicts an earlier phase of thinning coeval with Farallon slab removal.

The uncertainties in the estimates of past elevation and crustal thickness in the North American Cordillera persist because of limitations of existing methods for reconstructing these parameters back in time. For instance, the spatial and temporal resolution of stable isotope paleoaltimetry is limited by the availability of proxy material, which is often not preserved prior to the Cenozoic (L. Li et al., 2024; Licht et al., 2017; Quade et al., 2020). Interpretations of these data are often non-unique, requiring assumptions about paleo-temperature and relative humidity during moisture ascent, isotopic lapse rates, and sources of meteoric water to obtain quantitative estimates of past elevation (S. J. Davis et al., 2008; Galewsky, 2009; Lechler & Niemi, 2011; Rowley, 2007). While back-in-time strain integration studies provide high-resolution estimates of crustal thickness and elevation (Bahadori et al., 2018; Bahadori & Holt, 2019; Bahadori, Holt, Feng, et al., 2022), they do not account for open-system changes in crustal thickness that result from magmatic additions to the crust, crustal flow, or foundering of eclogitic lower crust, which were significant in the North American Cordillera (Block & Royden, 1990; DeCelles et al., 2009; DeCelles & Graham, 2015; Ducea & Saleeby, 1998; Gans, 1987; McQuarrie & Chase, 2000).

Recent advances in geochemical proxies of crustal thickness and elevation resolve some of these difficulties and enable high-resolution estimates of crustal thickness and paleoelevation that are independent of existing stable isotope or strain restoration studies. New calibrations also reduce uncertainty in paleoelevation and paleocrustal thickness results, enabling detection of lower-magnitude changes in these parameters through time. Here we apply these geochemical proxies to a compiled data set of 11,865 existing arc geochemical samples from the western North American Cordillera (Luffi & Ducea, 2022). Using this data set, we construct map-view visualizations of crustal thickness and elevation from the Late Cretaceous to Early Miocene. Adopting the regional classifications of Whitney et al. (2013) and J. B. Chapman et al. (2021), we generate time series of paleoelevation and crustal thickness in the southern (∼30–36°N), central (∼36–42°N), and northern (∼42–49°N) segments of the orogen. To test whether surface elevation is controlled by crustal thickness, we compare our results to previous stable isotope estimates of surface elevation. These analyses indicate the presence of a high-elevation (3–4 km), thick-crusted (∼50–60 km) highland that extended ∼1,500 km along strike at the onset of proposed Eocene–Oligocene slab foundering. In the central and southern segments of the North American Cordillera, high elevations and thick crust largely persisted until the onset of Basin-and-Range extension (ca. 17 Ma), implying that extensional collapse of the North American Cordillera was primarily achieved during post-Oligocene changes in plate boundary conditions.

2. Methods

The geochemical composition of arc magmas correlates with crustal thickness due to pressure-dependent differentiation at or near the base of the crust (Chiaradia, 2015; Dhuime et al., 2015; Farner & Lee, 2017; Hildreth & Moorbath, 1988; Mantle & Collins, 2008; Profeta et al., 2015; Turner et al., 2016). Empirical correlations between geochemical ratios and elevation or crustal thickness within modern arcs have been applied back in time to calculate these parameters within paleo-arcs. Most geochemical reconstructions have employed proxies that use a single or paired geochemical value or ratio, such as La/Yb or Sr/Y (e.g., J. B. Chapman et al., 2015; Profeta et al., 2015; Sundell et al., 2021), which necessarily limits the number of crustal thickness estimates that can be obtained. The calibration of 41 new depth to Moho proxies, or chemical mohometers, by Luffi and Ducea (2022) expands the quantity of estimates that can be derived from data within geochemical repositories, an advance that enables our methodological approach of reconstructing the spatial (i.e., map-view) patterns of crustal thickness through time (Liu et al., 2024). Previous single-proxy calibrations are also susceptible to systematic error related to processes independent of crustal thickness, including variability in geothermal gradients, source rock composition, disequilibrium garnet fractionation, and water activity (Kendrick & Yakymchuk, 2020; Lieu & Stern, 2019; Pourteau et al., 2020; Roberts et al., 2024). While the influence of these factors cannot be entirely excluded, chemical multi-mohometry results are better suited to isolating geochemical signatures attributable to crustal thickness from these confounding effects.

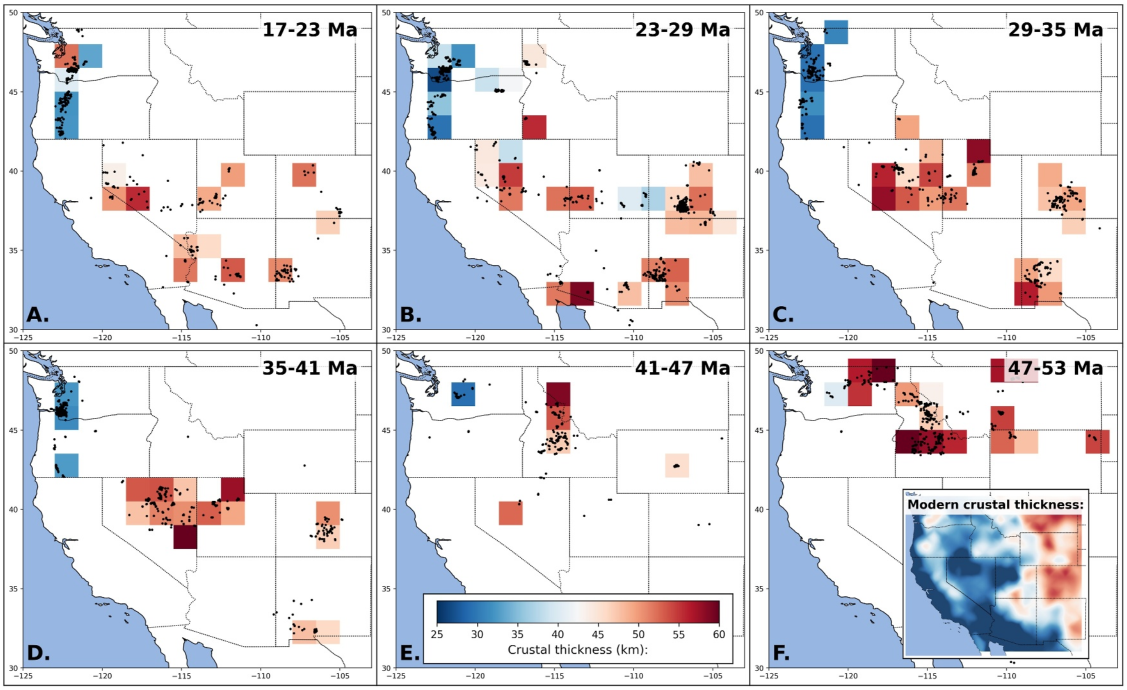

Figure 3. Maps of binned crustal thickness estimates from 53 to 17 Ma (a–f). Binned crustal thicknesses represent the median value within a 1.5° rectangle and a ±3 Ma moving window. See text for information about the binning methodology. Circles indicate the location of source data used in each map. The inset map in (f) shows modern crustal thickness using the same color scale (Laske et al., 2013).

2.1. Data Compilation

Whole-rock igneous geochemical data were downloaded from the EarthChem (https://portal.earthchem.org) and Western North American Volcanic and Intrusive Rocks (NAVDAT) databases for Late Cretaceous to Early Miocene (95–17 Ma) samples located west of 104°W longitude in the United States and northern Mexico (Ducea & Barton, 2007; Walker et al., 2006). Additional geochemical data were compiled from the literature (Best et al., 2009 and references therein; Biek, 2013; J. B. Chapman, Greig, & Haxel, 2020; Christiansen, 2009; Clark, 2007, 2015; Clark & Biek, 2017; Dudás et al., 2010; Feeley & Grunder, 1991; Gaschnig et al., 2011; Hiza, 1999; McKean, 2017; McKean et al., 2013; Nelson et al., 1998; Scarberry et al., 2021; Tepper et al., 2023; Valencia-Moreno et al., 2021 and references therein). Duplicates and samples with unreliable age or location information were excluded from the data set.

Samples were filtered to include only those produced in an arc setting. Samples derived from Basin-and-Range, slab-window (e.g., McQuarrie & Oskin, 2010), or Yellowstone hotspot volcanism are omitted by removing samples younger than 17 Ma from the data set. Units classified by J. B. Chapman et al. (2021) as part of the North American anatectic belt were also excluded, as crustal melts are not included in mohometry calibration data sets. We retain samples from the Idaho Batholith due to their origin in the Cordilleran arc. Samples classified as airfall tuffs were excluded because of the likely spatial offset between the volcanic source center and the sample location. Due to the prevalence of large ignimbritic eruptions in the western United States, samples classified as pyroclastic flows or ignimbrites were retained. The compiled data set consists of 11,865 samples from 444 publications (Figure 2; Table S1 in Supporting Information S2).

2.2. Crustal Thickness and Elevation Estimates

We use the Geochemical Arc Moho Estimator (GAME) tool to calculate crustal thickness and elevation from the compiled data set (Table S2 in Supporting Information S2; Luffi & Ducea, 2022). This tool calculates elevation as a function of the differentiation indicator MgO and a geochemical ratio or value using empirical regressions from modern (i.e., Pliocene–Holocene) arcs. Moho depth is then calculated from elevation using the regression: Moho depth (km) = 6.79 (±0.95) × elevation + 26.4 (±1.45), where Moho depth = crustal thickness – elevation.

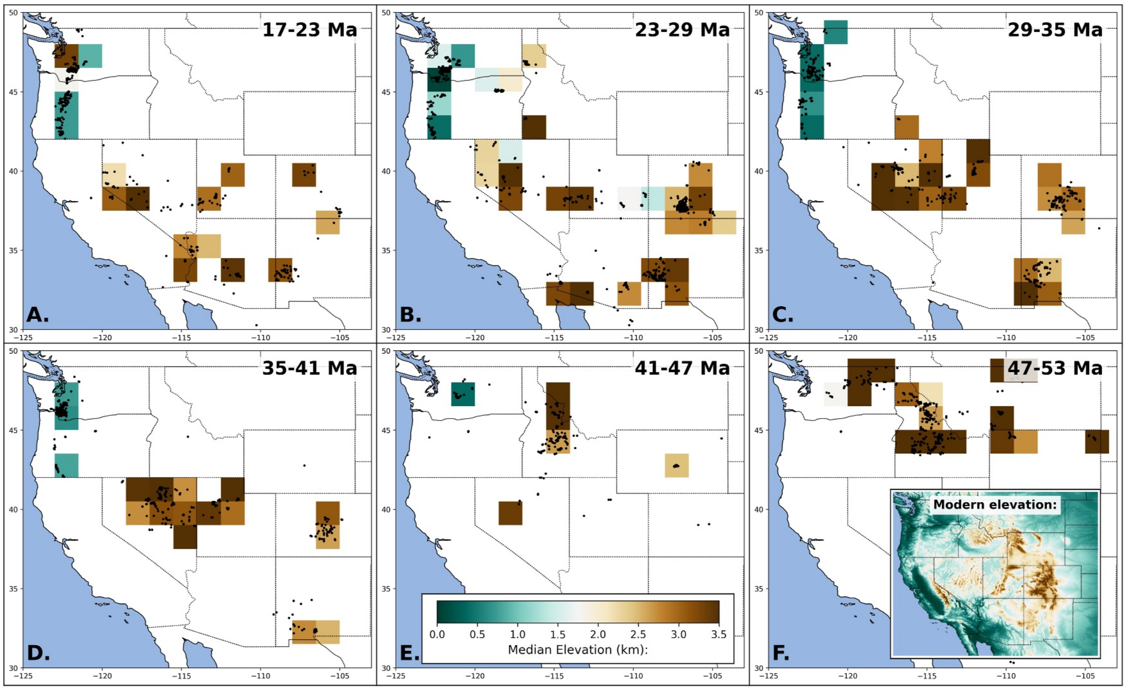

Figure 4. Maps of binned paleoelevation estimates from 53 to 17 Ma (a–f). Binned elevations represent median values within a 1.5° rectangle and a ±3 Ma moving window. See text for information about the binning methodology. Circles indicate the location of source data used in each map. The inset map in (f) shows modern elevation using the same color scale.

We completed two types of analyses to determine the spatial and temporal trends of crustal thickness and elevation in the North American Cordillera. First, we created maps of crustal thickness and elevation. This spatial perspective is enabled by the breadth of magmatism related to inboard and outboard sweeps as the Farallon slab flattened and subsequently rolled back (Coney & Reynolds, 1977). For all compiled samples that passed through data quality filters (major elements = 97%–101%; SiO_2 = 45%–80%; $Na_2O + K_2O$ less than 1.5% above the alkaline-subalkaline boundary), individual Moho depths were calculated using up to 41 calibrations in GAME. Mohometers with elevation calibration domain residuals (ε_{MAX} in Luffi & Ducea, 2022) greater than 1.0 km were excluded. To visualize spatial trends, median crustal thickness and elevation were calculated for 1.5° latitude and longitude bins using a ±3 Ma moving window. The spatial and temporal bounds of these bins were selected by an iterative approach that ensured a sufficient quantity of geochemical data within each temporal interval and bin while maintaining the resolution of estimates (e.g., Liu et al., 2024). Bins containing fewer than eight samples were discarded to avoid erroneous results. Results are presented as animations of Late Cretaceous to Early Miocene crustal thickness and elevation at 1 Ma intervals (Movies S1 and S2) and maps of Cenozoic time slices (Figures 3 and 4). Using these maps, we calculated the difference between modern crustal thickness and a Kriging interpolated surface of Early Miocene (17–23 Ma) crustal thickness (Figure 5) and median crustal thickness as a function of latitude and time for all data west of 109°W (Figure 6).

Second, we calculated three types of time series and point-in-time estimates of crustal thickness and elevation. Results for these analyses are reported as mean crustal thickness, and uncertainty bars indicate standard deviation. Model input parameters and results for these analyses are available in Tables S3–S5 in Supporting Information S2. (a) Time series of crustal thickness estimates and paleoelevation were constructed for three segments of the U.S. Cordillera: The southern Cordillera in Arizona (30–36°N), the central Cordillera in Nevada (36–42°N), and the northern Cordillera in eastern Washington, Idaho, and western Montana (42–49°N), corresponding with the inferred Arizonaplano (J. B. Chapman, Greig, & Haxel, 2020), Nevadaplano (DeCelles, 2004), and Montanaplano (Lageson et al., 2020). We subdivide each region into 3–4 subregions (Figure 2, black boxes) and calculate crustal thickness and elevation using GAME for geochemical data within each subregion at different time intervals. (b) Elevation and crustal thickness at the onset of MCC exhumation were calculated for eight MCCs or MCC clusters from southern Arizona to northern Washington (Figures 9; Figure 2, red boxes). While

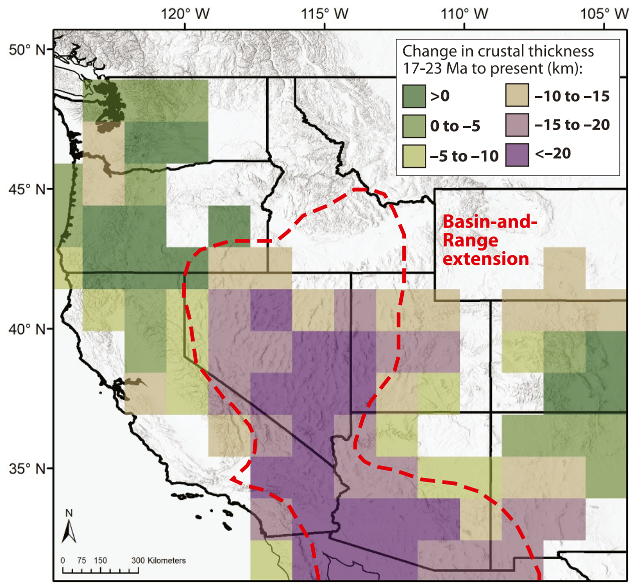

Figure 5. Map of changes in crustal thickness between the Early Miocene and the present, calculated by subtracting interpolated crustal thickness estimates within the 17–23 Ma time interval from modern crustal thickness (Laske et al., 2013). Negative values indicate a decrease in crustal thickness from the Early Miocene to the present. The red dashed line shows the approximate outline of the Basin-and-Range extensional province.

samples generally pre-date MCC exhumation in the central Cordillera, available geochemical data often post-date the onset of extension in the southern and northern regions, suggesting that crustal thickness estimates here may represent minimum values (e.g., Fayon et al., 2000; Howlett et al., 2021; Spencer et al., 2022). (c) To understand the controls on surface elevation, geochemical estimates of paleoelevation were compared to co-located and coeval estimates of paleoelevation from stable isotope paleoaltimetry (Figure 8). Paleoelevation estimates from chemical mohometry were calculated using geochemical data within a 100 km radius of each stable isotope estimate of paleoelevation (Figure 4). Stable isotope paleoaltimetry results often represent minimum elevations, as moisture mixing, surface evaporation, or moisture deflection can increase meteoric water δ^2H and δ^{18}O values. To ensure that paleoaltimetry results are directly comparable with chemical mohometry data, we use studies that report absolute paleoelevation. Since the quantification of paleoelevation estimates from stable isotope values relies on regional and proxy-specific considerations, we use elevation estimates reported within individual studies, except for two studies from central Nevada (Cassel et al., 2014, 2018) where we use paleoelevation estimates recalculated by Ibarra et al. (2021) using the Rayleigh distillation model of Rowley et al. (2001).

We here address several important caveats to our approach. First, map-view estimates of crustal thickness and elevation tend to be dispersed in regions where geochemical data are sparse. For this reason, we regard our time-series estimates (Figure 7), which incorporate a mean of 87 samples per data point (range of 14–277), as a more robust record of crustal thickness and prioritize these results in our interpretations. Second, the availability of geochemical samples and the precision of sample ages decrease in the early Cenozoic and Cretaceous relative to the mid and late Cenozoic (17–55 Ma: $n = 9{,}254$, median uncertainty = 2.4 Ma; 55–95 Ma: $n = 2{,}611$, median uncertainty = 6.6 Ma). As such, we focus our discussion on the Cenozoic record of crustal thickness and paleoelevation. Third, chemical mohometry results assume crustal isostatic equilibrium and do not account for dynamic or non-crustal isostatic effects (e.g., removal of mantle lithosphere or fluid-driven de-densification of lithosphere). In modern arcs, crustal thickness is the primary control on surface elevation (e.g., Beck et al., 1996; Farner & Lee, 2017; Luffi & Ducea, 2022). As

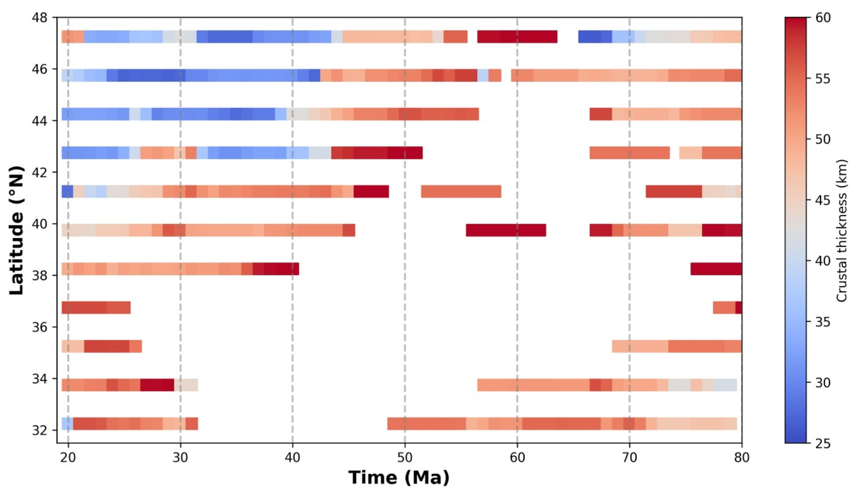

Figure 6. Crustal thickness as a function of latitude and time. Plotted values correspond to the midpoint of a ±3 Ma moving window of binned data. For each interval, crustal thickness is calculated as the average of all bins west of 109°W along a line of latitude, which excludes data from Colorado, New Mexico, eastern Montana, and central and eastern Wyoming. Between 40° and 48°N, the Eocene shift to thinner crust corresponds to the cessation of most volcanism in Idaho and Montana and the initiation of the Cascades arc to the west.

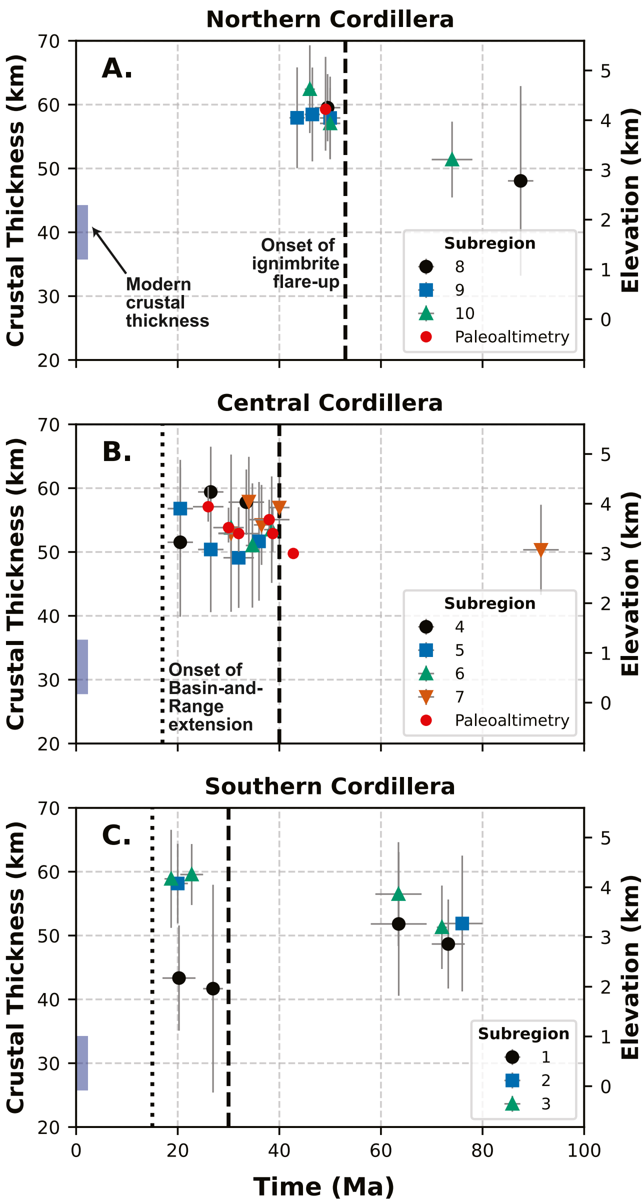

Figure 7. Time series of mean crustal thickness and elevation for the (a) northern, (b) central, and (c) southern Cordillera. Results represent crustal thickness and elevation within subregions in Figure 2 calculated using the Geochemical Arc Moho Estimator tool (Luffi & Ducea, 2022). A mean and median of 87 and 58 arc geochemical samples, respectively, are used to calculate each data point. Red circles indicate results from existing stable isotope paleoaltimetry studies while dashed lines indicate the approximate timing of Basin-and-Range extension and volcanism during the "ignimbrite flare-up" within each region. Crustal thickness uncertainty bars indicate the standard deviation.

discussed below, we evaluate this assumption in the past by comparing geochemical estimates of elevation with coeval and co-located estimates of surface elevation from stable isotope paleoaltimetry data (Figure 8).

The uncertainty of individual geochemical values remains unquantified in our data compilation. To determine the influence of this uncertainty on Moho depth and elevation results, we performed a Monte Carlo analysis using representative geochemical data from the central Cordillera (region 7 in Figures 2, 35–38 Ma). We derived 100 synthetic data sets by sampling normal distributions created using each geochemical value as a mean and 3% as the standard deviation. Each synthetic data set was then input into GAME to quantify how uncertainty in geochemical input values may influence model outputs. Model outputs yield mean Moho depth estimates with a standard deviation of 0.8 km and elevation estimates with a standard deviation of 0.1 km (Table S6 in Supporting Information S2). Thus, output uncertainty from uncertainty in input geochemical values appears to be relatively small, and secondary to other quantified sources of uncertainty in our analysis.

3. Regional Results and Interpretations

We first discuss results within the northern, central, and southern regions of the North American Cordillera (Figure 2), and compare new elevation and crustal thickness estimates to existing constraints from structural, stable isotope, stratigraphic, and geochemical studies. We next examine the implications of our results for the orogen-scale geometry of the North American Cordilleran highland, the drivers of Cenozoic extensional collapse, and the mechanisms responsible for the development and support of high topography. We then discuss the link between crustal thickness and the formation of metamorphic core complexes.

3.1. Northern Cordillera

Crustal thickness results indicate the presence of a Cenozoic orogenic highland in the western Montana and Idaho portions of the Cordillera with mean crustal thicknesses of 58.9 km and paleoelevations of 4.2 km (Figures 3, 4, and 7a) during the Eocene. This feature (the Montanaplano of Lageson et al., 2020) was likely a northward continuation of the Nevadaplano, consistent with a variety of previous constraints on paleoelevation and crustal thickness. Stable isotope data indicate high elevations adjacent to the Sage Creek and Kishenehn basins (Fan et al., 2017; Mix et al., 2011) during the early Eocene, and paleoaltimetry results elsewhere in the Idaho and Montana Cordillera are consistent with high Eocene paleoelevations ranging from 3 to 5 km (Chamberlain et al., 2012; Kent-Corson et al., 2006; Mulch et al., 2007; Schwartz et al., 2019). Northeast-dipping fabrics in the Bitterroot lobe of the Idaho Batholith have been interpreted as evidence of contraction during crustal thickening (Byerly et al., 2017), while a shift toward more evolved radiogenic isotope values through time indicates increased crustal melting resulting from crustal thickening (J. B. Chapman et al., 2021; Gaschnig et al., 2011). Thermobarometry estimates of the Idaho Batholith indicate emplacement depths of ∼12 km, which require crustal thicknesses of 52–57 km during emplacement given modern crustal thicknesses of 40–45 km (Byerly et al., 2017; Jordan, 1994; Laske et al., 2013).

On the eastern margin of this highland, a series of east- and southeast-draining paleovalleys were incised during the Late Cretaceous (Chetel et al., 2011; Janecke et al., 2000), analogous to a system of Cretaceous paleovalleys from the central Cordillera (Henry, 2008; Henry et al., 2012). Paleovalley development and erosion on the eastern

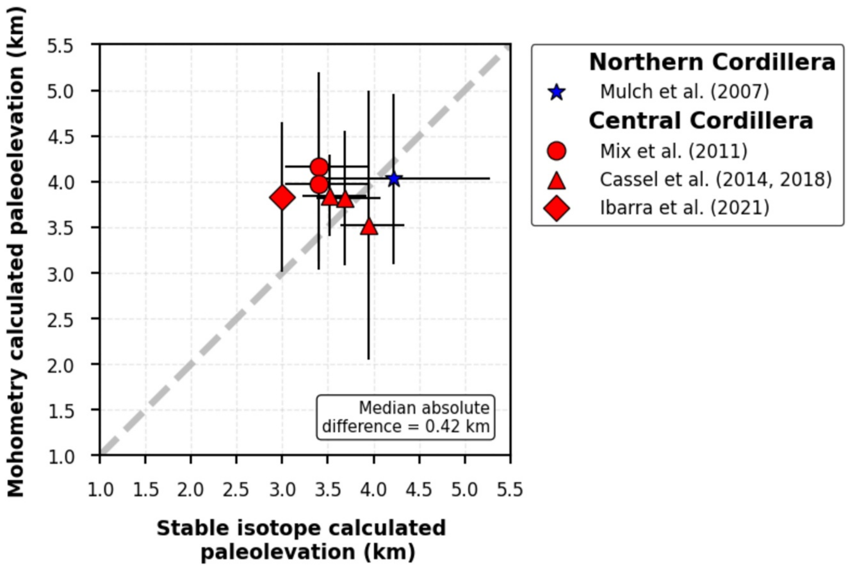

Figure 8. Plot of paleoelevation estimated from stable isotope paleoaltimetry (Cassel et al., 2014, 2018; Ibarra et al., 2021; Mix et al., 2011; Mulch et al., 2007) versus co-located and coeval estimates of mean paleoelevation calculated from chemical mohometry. See Table S5 in Supporting Information S2 for source data. Mohometry calculated paleoelevation uncertainty bars indicate the standard deviation of the mean.

margin were likely enhanced by a strong west-directed monsoon originating from the Cretaceous Western Interior Seaway (Foreman et al., 2011; Fricke et al., 2010; Lageson et al., 2020).

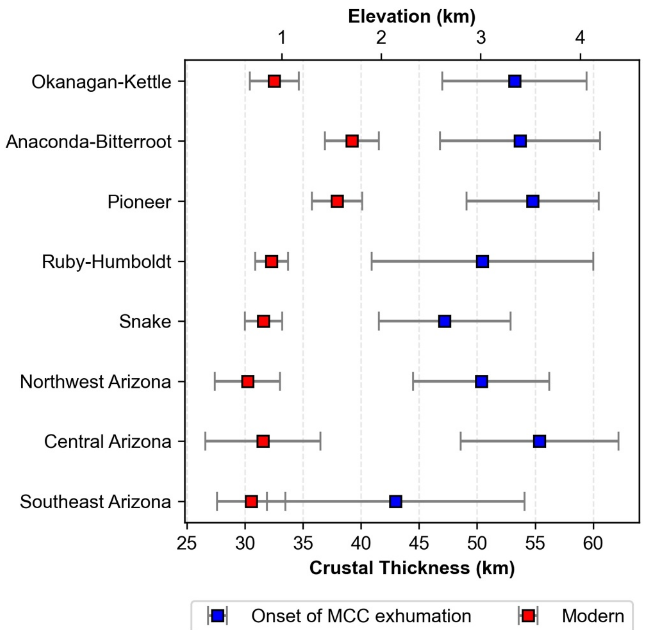

Figure 9. Mean crustal thickness and elevation at the onset of metamorphic core complex (MCC) exhumation for eight clusters of MCCs. Red squares indicate modern crustal thickness from Laske et al. (2013). See Figure 2 for the locations of geochemical data for each metamorphic core complex or cluster of metamorphic core complexes. Uncertainty bars of crustal thicknesses indicate the standard deviation of the mean.

Similar to the Nevadaplano, crustal thickening in Idaho and Montana was likely driven by Cretaceous and early Cenozoic shortening. Balanced cross sections from southern Alberta (~50°N; Price, 1981), northwest Montana (~48°N; Fuentes, 2012), and Wyoming and southern Idaho (~42°N; Coogan, 1992) document an average of 182 km of minimum shortening, similar to estimates of 150 and 222 km from northern and central Utah, respectively (Coogan, 1992; DeCelles & Coogan, 2006). We interpret this along-strike consistency in the magnitude of retro-arc shortening to indicate that an orogenic highland in the central and northern Cordillera was a north–south-trending, spatially continuous physiographic feature. Crustal thickening may have also been locally driven by magmatism during emplacement of voluminous plutons, such as the 6,000 km^2 Boulder batholith (Lageson et al., 2001; Vejmelek & Smithson, 1995).

Crustal thickness results do not show detectable crustal thinning from ca. 53 to 43 Ma (Figure 7a), and a lack of available geochemical data thereafter precludes reconstruction of the timing and rate of crustal thinning from peak Eocene thicknesses (~58 km) to modern thicknesses (40–45 km). Surficial and thermochronologic evidence suggests this crustal thinning occurred through a combination of post-orogenic Paleogene extension, including via reactivation of thrust faults, Neogene Basin-and-Range extension, and extension related to the impingement of the Yellowstone hotspot (Camp et al., 2015; Constenius, 1996; Janecke, 1994; Schwartz & Schwartz, 2013; Thoresen et al., 2024; Wernicke, 1992).

Following the accretion of the Siletzia oceanic plateau and the cessation of magmatism in the interior of the orogen, subduction re-initiated to the west to form the Cascades arc ca. 45 Ma (Schmandt & Humphreys, 2011; Tepper & Clark, 2024). Our results indicate that the Cascades had relatively thin crust

(~30 km) and low (<1 km) paleoelevations during the Eocene and earliest Oligocene (Figures 3 and 4). This result aligns with evidence that the early Cascades arc consisted of a discontinuous chain of low-elevation, sub-aqueous to sub-aerial volcanic centers separated by large along-strike gaps in volcanism (Du Bray & John, 2011; Hammond, 1979; Jutzeler et al., 2014; Methner et al., 2016). The early arc lacked a retro-arc fold-and-thrust belt, and may have experienced a phase of early Oligocene slab rollback, consistent with the observation of relatively thin arc crust until at least the early Oligocene (Basler & Cassel, 2025; Humphreys & Grunder, 2022; Priest, 1990). In this scenario, the early Cascades represented a thin-crusted, weakly convergent endmember continental arc, in contrast to the strongly convergent Cordilleran-type orogenic system that previously characterized the margin.

3.2. Central Cordillera

Crustal thickness results from the central segment of the Cordillera indicate the late Paleogene–early Neogene (ca. 39–20 Ma) presence of the Nevadaplano orogenic plateau with mean crustal thickness of 54.0 km and elevation of 3.5 km (Figures 3, 4, and 7b). Although generally overlapping with previous estimates of crustal thickness in the region (Bahadori et al., 2018; J. B. Chapman et al., 2015; Coney & Reynolds, 1977; DeCelles & Coogan, 2006; Konstantinou, 2022; Long, 2019, 2023; Lund Snee & Miller, 2022), these estimates diverge from suggestions that the crust was up to 70 km thick (Best et al., 2009, 2016).

Across the four subregions, mean estimates of crustal thickness are clustered around 54 km between the late Eocene and Early Miocene. A plausible explanation for this uniformity in crustal thickness estimates is the reduction of Moho topography via the lateral flow of lower or mid crust (Bird, 1991), consistent with the view that the Cenozoic Nevadaplano was a high-elevation region with low internal relief (Best & Christiansen, 1991; DeCelles, 2004; Henry, 2008). The low-angle unconformity between Cenozoic volcanic rocks and Paleozoic strata in eastern Nevada and western Utah provides additional evidence of a plateau-like setting (Armstrong, 1972; DeCelles, 2004). Progressive topographic smoothing during emplacement of successive ignimbrite sheets may have contributed to further reductions in internal relief during late Eocene to Early Miocene volcanism (Best et al., 2009).

While the existence of plateau-like topography in the central Nevada hinterland is well-documented, the along-strike continuity of this plateau to the southern portion of the Cordillera remains unclear. The paleo-width of the hinterland was likely narrower in western Arizona and far southern Nevada (Jones, 2025), which may preclude the existence of a broad, plateau-like feature comparable to central Nevada. Strain restoration studies also reconstruct a narrower highland in Arizona relative to areas further north (Bahadori, Holt, Feng, et al., 2022; Bahadori et al., 2018). This region was actively eroding in the Late Cretaceous and early Cenozoic, and may have represented the sediment source of several regional drainages and basins (Caylor et al., 2021; Dickinson, 2012; Kapp et al., 2023; Sharman et al., 2017). These data sets do not appear compatible with a wide, plateau-like region and suggest that significant topographic heterogeneity may have been present in western and southern Arizona.

In all four central Cordillera subregions (Figure 2), Paleogene through early Neogene crustal thickness does not change within the uncertainty of mohometry estimates. This result suggests that the crust remained relatively thick until the Early Miocene, and that most crustal thinning was achieved via Basin-and-Range extension beginning at ca. 17 Ma (Colgan & Henry, 2009). This lack of Eocene–Oligocene thinning of the crust in Nevada and western Utah aligns with several lines of evidence: Sedimentologic studies indicate the lack of a significant basin record of pre-Miocene normal faulting (Best & Christiansen, 1991; Henry et al., 2011), long run-out distances of ignimbrites attest to low-relief topography that had yet to be dissected by surface-breaking faulting (Best et al., 2016), thermochronologic data indicate most ranges were not exhumed until the Miocene (E. L. Miller et al., 1999; Zuza, Jepson, & Cao, 2024), and elongated E–W aspect ratios of calderas suggest extension post-dated volcanism. In the eastern Nevadaplano, work suggests that normal faulting and corresponding deposition occurred during the Eocene–Oligocene, which could indicate that limited crustal thinning initiated prior to the Miocene onset of Basin-and-Range-style extension (Constenius, 1996; Evans et al., 2015; Gans et al., 1989; Henry et al., 2011; J. Lee et al., 2017; Long, 2019; Long & Walker, 2015). Our results suggest that this initial phase of extension, which may have been limited in areal extent and magnitude, did not result in sufficient crustal thinning to be detectable using paleocrustal thickness proxies (Figure 7b).

Within uncertainty, paleoelevation results from chemical mohometry are similar to coeval stable isotope studies of Paleogene surface elevation (Figures 7b and 8; Cassel et al., 2014, 2018; Ibarra et al., 2021). Elevation estimates from arc geochemical proxies and stable isotopes are sensitive to different processes (i.e., lithospheric vs. atmospheric archives of elevation), and agreement between these independent methods provides strong evidence that high elevations persisted until the late Oligocene to Early Miocene.

3.3. Southern Cordillera

Estimates of crustal thickness from southern Arizona and northern Mexico indicate that moderately thick crust and high paleoelevations developed by the early Cenozoic (Figures 3, 4, 6, and 7c). This region (the Arizonaplano of J. B. Chapman, Greig, & Haxel, 2020) featured mean Cenozoic crustal thicknesses of 52.8 km and mean paleoelevations of 3.4 km, in broad agreement with previous geochemical reconstructions of crustal thickness (J. B. Chapman, Greig, & Haxel, 2020; Jepson et al., 2022) and results from integrating strain rates back in time (Bahadori & Holt, 2019; Bahadori, Holt, Feng, et al., 2022; Bahadori et al., 2018).

The mechanisms responsible for thickening the crust may vary within the region. In western Arizona and far eastern California, crustal thickening ca. 70–90 Ma was driven by shortening in the Maria fold-and-thrust belt (MFTB), a basement-involved but thin-skinned ductile thrust belt that strikes east-west and verges south, in contrast to the general eastward vergence of most Sevier-style shortening (Barth et al., 2004; Knapp & Heizler, 1990; Salem, A. C., 2009; Spencer & Reynolds, 1990). Following the cessation of shortening in the Late Cretaceous, thickening in the region may have occurred through the northeastward translation of lithospheric material by the flat Farallon slab (Axen et al., 2018; A. Chapman, Shields, et al., 2020; Kapp et al., 2023; Rautela et al., 2020) or through emplacement of subducted Pelona, Orocopia, and Rand schists (A. D. Chapman, 2017; Seymour et al., 2018). Superimposed on these processes is the possibility of magmatic thickening via the Late Cretaceous and early Cenozoic emplacement of Laramide plutons (Erdman et al., 2016).

The mechanisms of crustal thickening east of the Maria fold-and-thrust belt remain less certain. Thrust faults in this region are generally interpreted as high-angle structures with limited offset (e.g., G. H. Davis, 1979; Favorito & Seedorff, 2021), which could not contribute to significant crustal thickening. Our results suggest that crustal thicknesses during both the Late Cretaceous–Paleocene and Oligocene–Miocene were lower in southeastern Arizona relative to western and central Arizona, a discrepancy which could reflect a difference in the magnitude of shortening. Nonetheless, some low-angle thrusts have been recognized in eastern Arizona, implying that shortening could represent an under-appreciated mechanism of crustal thickening (Bykerk-Kauffman & Janecke, 1987; J. B. Chapman et al., 2025; Dickinson, 1991; Gehrels & Smith, 1991).

New estimates of Oligocene and Early Miocene crustal thickness in the southern Cordillera provide constraints on the mechanisms through which this highland thinned to modern crustal thicknesses of ∼30 km (Figure 3, inset map; Laske et al., 2013; Shen & Ritzwoller, 2016; Jepson et al., 2022). Results indicate crustal thicknesses of 59 ± 8, 58 ± 6, and 43 ± 8 km in western, central, and southeast Arizona, respectively, at ca. 20 Ma (Figure 9). Assuming maximum crustal thicknesses of ∼55–60 km, these results imply that limited thinning occurred prior to the onset of Basin-and-Range extension in western and central Arizona (Jepson et al., 2022).

The observation of relatively thick crust in the Early Miocene is difficult to reconcile with evidence that significant extension began in the Oligocene in Arizona (J. B. Chapman et al., 2024; Fayon et al., 2000). This discrepancy may in part reflect diachronous extension across the region: Thinner crust at ca. 20–30 Ma in southeastern Arizona relative to areas farther northwest may be consistent with an earlier onset of extension (ca. 30 Ma) in the Catalina-Rincon, Pinaleño, and Coyote metamorphic core complexes relative to areas farther west, which hosted thicker crust (J. B. Chapman et al., 2024; Fayon et al., 2000; Gottardi et al., 2020; Spencer et al., 2022). Extension in metamorphic core complexes may be relatively slow (e.g., Buck, 1991), and initially occur along high-angle faults (Kapp et al., 2008), both of which would limit the degree of crustal thinning following the onset of exhumation.

Two additional mechanisms may have been important in maintaining relatively thick crust after the onset of extension. First, mid-crustal flow during metamorphic core complex exhumation may offset upper crustal extension during detachment faulting. During MCC exhumation, upper-crustal unloading produces a lateral pressure gradient in the crust, driving crustal flow toward the locus of extension (Block & Royden, 1990). Upper crustal extension is thus in part compensated by lower crustal flow, attenuating the degree of local crustal thinning. The observation of a modern flat Moho beneath MCCs supports this interpretation, since upper-crustal extension during MCC exhumation should locally thin the crust absent crustal flow. The ability of the lower crust to flow in the Oligocene in Arizona is supported by the existence of syn-rollback Oligocene–Miocene crustal melting, which may reflect the exposure of upper plate lithosphere to hot asthenosphere following the foundering of the Farallon slab, along with radiogenic heating of previously thickened crust (J. B. Chapman et al., 2021, 2023; Dombroski & Fodor, 2019). Second, the crust may have been locally thickened through Oligocene and Miocene magmatism. Foundering of the Farallon flat slab drove volcanism throughout the western U.S. during the "ignimbrite flare-up," which migrated into southern Arizona by ca. 28 Ma (Armstrong & Ward, 1991; McQuarrie & Oskin, 2010). Flare-up volcanism corresponded to the input of voluminous mantle basalt into the crust, which may have provided an important mechanism to maintain or thicken the crust during initial extension along low-angle detachment faults (Farmer et al., 2008; Gans, 1987; Johnson, 1991; Konstantinou, 2022; G. Li et al., 2022; Lipman, 2021).

4. Cordilleran-Wide Interpretations

New chemical mohometry results indicate that a spatially continuous Late Cretaceous-Paleogene orogenic highland extended ~1,500 km along strike (~30–49°N; Figures 3 and 4, Movies S1 and S2). Geochemical evidence for this feature is independent of most previous efforts to reconstruct the crustal thickness and paleoelevation of the orogen, particularly in the northern segment of the Cordillera. High elevations and thick crust likely extended farther south (J. B. Chapman, Greig, & Haxel, 2020) and north (Brown & Gibson, 2006; Mulch et al., 2007; Teyssier et al., 2005) of our study area, consistent with a minimum along-strike distance of 1,500 km. Between 30 and 49°N, the Cenozoic orogenic hinterland was characterized by average crustal thicknesses of 54.8 km and paleoelevations of 3.6 km, with maximum crustal thickness and paleoelevation of 62.4 and 4.6 km, respectively. Paleogene crustal thicknesses were highest (~55–60 km) in the northern Cordillera and the western Arizona portion of the southern Cordillera, and slightly lower (~50–56 km) in the central portion of the Cordillera. The spatial extent of this thickened crust corresponds to the footprint of Cretaceous–Cenozoic crustal anatexis, which may imply that prolonged radiogenic heating of thickened crust contributed to crustal melting (J. B. Chapman et al., 2021; C. F. Miller & Bradfish, 1980).

4.1. Mechanisms of Topographic Support

Proposed controls on the development and support of elevated topography in Cordilleran hinterlands can be partitioned into two endmember models. The first model emphasizes the role of incremental crustal thickening in constructing an orogenic plateau through shortening in the retro-arc fold-and-thrust belt (DeCelles, 2004). While not necessarily ruling out crustal thickening and shortening as a key component of highland development, the second model argues that more abrupt processes, such as removal of eclogitic arc roots and/or mantle lithosphere, are the primary factors controlling surface elevation (Ducea, Chapman, Bowman, & Balica, 2021; Ducea, Chapman, Bowman, & Triantafyllou, 2021; Erdman et al., 2016; Garzione et al., 2008). In the North American Cordillera, this latter model has been invoked as the driver of large-magnitude (>2 km), diachronous surface uplift during south-directed foundering of the Farallon slab, which may have resulted from a combination of delamination of mantle lithosphere, heating of mantle lithosphere, or dynamic uplift (Chamberlain et al., 2012; Horton, 2004; Mix et al., 2011; Roy et al., 2009; Schwartz et al., 2019). Prior Late Cretaceous or early Cenozoic de-densification of crust or mantle lithosphere through the release of fluids from the subducting slab may represent an additional mechanism of topographic support that is independent of shortening-driven crustal thickening (Butcher et al., 2017; Humphreys et al., 2003; Jones et al., 2015).

Chemical mohometry data can be compared with existing estimates of paleoelevation to evaluate the mechanisms supporting high elevations. Since correlations between arc geochemistry and surface elevation reflect pressure-dependent processes at or near the base of the crust, paleoelevation estimates from chemical mohometry primarily represent the component of surface elevation produced via crustal isostasy (Farner & Lee, 2017; C.-T. A. Lee et al., 2015; Luffi & Ducea, 2022). By contrast, estimates of paleoelevation from stable isotopes reflect the actual magnitude of surface elevation, which is the integrated signal of flexural, dynamic, and isostatic topography, including isostatic processes that are not controlled by crustal thickness (e.g., delamination of mantle lithosphere or thermally driven changes in lithospheric density). These differences in the sensitivity of each proxy to the mechanisms of topographic support can be exploited to reconstruct the first-order mechanisms controlling past surface elevations.

Such comparisons between stable isotope paleoaltimetry and chemical mohometry data, however, require careful consideration of the spatial and temporal sensitivity of each proxy. Chemical mohometry results likely record pressure conditions across tens of km over several Ma (Luffi & Ducea, 2022). While paleo-precipitation stable isotope values typically have shorter integration times, most compiled data represent averages of several samples, limiting the effects of shorter-term isotopic variability. Spatially, stable isotope paleoaltimetry data are sensitive to upwind rainout along the moisture trajectory (Rowley, 2007). In leeward tectonic settings, these data can reflect the elevation of upwind topography, rather than local elevation, which may preclude comparison with co-located chemical mohometry data (Blisniuk & Stern, 2005). However, most stable isotope data compiled here were generally located near the crest of a hinterland paleo-highland, suggesting that these results are likely local elevations, rather than the elevation of distant upwind topography. This interpretation is consistent with reconstructed paleo-drainages in the central Cordillera, and isotope evidence that elevation-driven rainout occurred progressively across the Nevadaplano (Cassel et al., 2014, 2018; Henry et al., 2012).

New comparisons between chemical mohometry-estimated paleoelevations and absolute estimates of paleoelevation from stable isotope paleoaltimetry (Figure 8) agree within uncertainty (median absolute difference = 0.4 km). Due to the uncertainties of both methods, this result does not exclude the possibility of smaller-magnitude dynamic, thermal, or flexurally-supported topography during rollback of the Farallon slab (Bahadori & Holt, 2019; Cassel et al., 2018; Smith et al., 2017). However, this result appears incompatible with large-magnitude (>2 km) surface uplift at this time (Mix et al., 2011; Schwartz et al., 2019) resulting from dynamic processes, the heating and de-densification of mantle lithosphere, or delamination of mantle lithosphere, which would predict a detectable offset between stable isotope and chemical mohometry estimates of paleoelevation.

4.2. Implications for Cenozoic Extension in the Southern and Central Cordillera

Our results indicate that the crust remained relatively thick until the Early Miocene and late Oligocene in the central and southern segments of the North American Cordillera (Figures 5 and 7; mean = 53.7 km at ca. 20 Ma), with the exception of thinner crust in southeastern Arizona. Since the availability of pre-Eocene geochemical data in the Sevier hinterland is limited, we cannot exclude the possibility of crustal thinning prior to foundering of the Farallon slab, which would make our Eocene–Miocene estimates of the elevation and crustal thickness of the Cordilleran hinterland minima (Hodges & Walker, 1992; Long et al., 2015; Long & Kohn, 2020; Wells & Hoisch, 2008; Wells et al., 1990, 2012). However, this earlier phase of Cretaceous and early Cenozoic syn-convergent extension is distinct from subsequent mid- to late Cenozoic extension associated with detachment faults and higher-angle Basin-and-Range-style faulting (Best & Christiansen, 1991; Dickinson, 1991).

The persistence of thick crust until at least the Early Miocene imposes several constraints on the potential drivers of crustal thinning (Colgan & Henry, 2009; Sonder & Jones, 1999). Given the lack of detectable crustal thickness change associated with rollback of the Farallon slab and exposure of upper plate lithosphere to warm asthenosphere, our results suggest that thermal weakening during Farallon slab rollback was insufficient to drive immediate, large-magnitude crustal thinning. Similarly, lithospheric buoyancy acquired during slab foundering, from delamination of mantle lithosphere or lithospheric heating (Bahadori & Holt, 2019), does not appear to be a significant driver of orogenic collapse, given the lack of coeval thinning and agreement between paleoelevations calculated via chemical mohometry and stable isotope paleoaltimetry (Figure 8). We cannot exclude the possibility of limited pre-Miocene crustal thinning within the uncertainty of our chemical mohometry results. As noted above, magmatic additions to the crust may have also been an important mechanism of crustal thickening that could have locally offset initial thinning during syn-magmatic extension.

Since thick hinterland crust developed by the Late Cretaceous and early Cenozoic, at least 30 Ma prior to the onset of widespread extension in western Arizona and southern Nevada, the mid to early Cenozoic collapse of overthickened crust was not the proximate driver of crustal thinning, although positive gradients in gravitational potential energy associated with this thick crust likely facilitated later extension (Dewey, 1988; Long, 2019). Instead, the synchroneity between the onset of extension and a transition to a transform plate margin implies that a change in plate boundary conditions was necessary to initiate significant extension, especially given the ca. 17 Ma expansion of the margin following the subduction of several microplates (Colgan & Henry, 2009). Thus, we favor a model in which most crustal thinning in the central and southern Cordillera was temporally associated with a change in boundary conditions along the western North American plate margin.

4.3. Implications for Metamorphic Core Complexes

New results of crustal thickness at the onset of MCC exhumation indicate that MCCs formed within thick or moderately thick crust in the North American Cordillera (Figure 9; Bahadori, Holt, Austermann, et al., 2022; Coney & Harms, 1984; Mulch et al., 2007). Estimates of crustal thickness for eight MCCs and MCC clusters (Figure 2) average 54.6 ± 4.9 km (elevation = 3.6 ± 0.6 km; uncertainty represents the standard deviation of mean values) with seven of eight MCCs featuring average thicknesses of >50 km and one (SE Arizona cluster) with slightly lower crustal thicknesses (45.4 ± 12.7 km). These estimates of crustal thickness are likely minima, as available geochemical data at some MCCs post-date the onset of exhumation by several Myr. Our results suggest that moderately thick crust is a likely prerequisite for the formation of metamorphic core complexes in the North American Cordillera, consistent with strain restoration (Bahadori & Holt, 2019; Coney & Harms, 1984) and modeling studies (Buck, 1991). The link between thick crust and MCC formation likely reflects a combination of buoyancy forces and decoupling between upper and lower crust as a result of post-thickening heating (Armstrong & Ward, 1991; Buck, 1991; Tirel et al., 2008; Whitney et al., 2013; Wijns et al., 2005). Relatively steep geothermal gradients within thick crust may promote lower or mid-crustal flow, preventing the development of Moho topography and localizing strain along a detachment fault (Block & Royden, 1990; Gans, 1987; Wernicke, 1992).

Beyond the first-order control of crustal thickness on MCC formation, recent work has linked crustal thickness to the variable spacing of metamorphic core complexes in western North America (Levy et al., 2023; Zuza & Cao, 2023; Zuza, Cao, et al., 2024; Zuza, Jepson, & Cao, 2024). This model suggests that MCCs west of the Sevier fold-and-thrust front formed within thick (~55 km) hinterland crust, while those farther to the south and east in Arizona and northern Mexico formed within thinner (~40 km) foreland crust. This inferred difference in crustal thickness was interpreted to cause shorter-wavelength Rayleigh-Taylor instabilities in the foreland, explaining the observation that foreland MCCs are more closely spaced than hinterland MCCs. New crustal thickness results indicate that hinterland MCCs had mean crustal thicknesses (55.9 ± 6.2 km; $n = 5$) indistinguishable from foreland MCCs (53.0 ± 7.2 km; $n = 3$) at the onset of extension, which deviates from the 15 km difference necessary to explain MCC spacing in this model. Thus, we do not find evidence that a spatial difference in crustal thickness can account for the observed differences in MCC spacing, implying that mechanisms separate from a diapiric Rayleigh-Taylor instability may be necessary to explain this variable spacing. In the Colorado River Extensional Corridor, the spacing of MCCs may instead reflect the geomorphic expression of antiformal footwall corrugations, which form individual ranges bounded by basins above corresponding footwall synforms (e.g., Singleton, 2013).

5. Conclusions

We calculated crustal thickness and elevation of the western North American Cordillera from the Late Cretaceous to Miocene (95–17 Ma) by applying new geochemical proxies to a compilation of arc geochemical data. We also calculated crustal thickness at the onset of metamorphic core complex exhumation and compared geochemically derived estimates of elevation to existing stable isotope paleoaltimetry results. Our new maps and time series of past crustal thickness and elevation indicate:

1. At the ca. 53 Ma onset of Farallon slab foundering, a continuous orogenic highland likely extended at least 1,500 km along-strike (~30°–49°N), from southern Arizona to northern Idaho and Montana. This region was characterized by crustal thicknesses between 50 and 60 km (mean = 54.8 km) and paleoelevations between 3 and 4 km (mean = 3.6 km).
2. Crustal thicknesses at the onset of exhumation for eight MCCs were ~55 km, indicating that thick to moderately thick crust likely represents a precondition for MCC formation.
3. Crustal thickness estimates from central Nevada to central Arizona indicate that the hinterland maintained moderately thick crust (~50–55 km) until the ca. 17 Ma onset of Basin-and-Range extension, suggesting that most thinning post-dated rollback of the Farallon slab. We favor a model that implicates a change in plate boundary kinematics during subduction of an oceanic spreading center as the cause of significant crustal thinning.
4. Paleoelevation estimates from chemical mohometry overlap within uncertainty with previous stable isotope estimates of paleoelevation. This result is incompatible with large-magnitude (>2 km) syn-rollback uplift via dynamic topography, thermally driven changes in lithospheric density, and/or delamination of mantle

lithosphere, though the modest uncertainties of both methods permit more limited changes in surface elevation resulting from these mechanisms.

Conflict of Interest

The authors declare no conflicts of interest relevant to this study.

Data Availability Statement

Compiled geochemical data and sample-level results are available in Tables S1–S6 in Supporting Information S2 and at https://doi.org/10.5281/zenodo.18078382 (Basler et al., 2026).

Acknowledgments
This work was supported by graduate student grants to LCB from the Geological Society of America, Peter Coney Scholarship, Sulzer Scholarship, and Pierce Scholarship. MND acknowledges funding of project #64 by the program PNRR-III-C9-2023–I8 of the Romanian MCID (64/30.07.2023) and project PN-IV-P1-PCE-2023-0204 funded by UEFISCDI. We thank Tyler Grambling, an anonymous reviewer, and associate editor Alexis Ault for constructive feedback.

References

Armstrong, R. L. (1972). Low-angle (denudation) faults, hinterland of the Sevier orogenic belt, eastern Nevada and western Utah. *Geological Society of America Bulletin*, *83*(6), 1729–1754. https://doi.org/10.1130/0016-7606(1972)83[1729:ldfhot]2.0.co;2

Armstrong, R. L., & Ward, P. (1991). Evolving geographic patterns of Cenozoic magmatism in the North American Cordillera: The temporal and spatial association of magmatism and metamorphic core complexes. *Journal of Geophysical Research*, *96*(B8), 13201–13224. https://doi.org/10.1029/91JB00412

Atwater, T. (1970). Implications of plate tectonics for the Cenozoic tectonic evolution of western North America. *Geological Society of America Bulletin*, *81*(12), 3513–3536. https://doi.org/10.1130/0016-7606(1970)81[3513:ioptft]2.0.co;2

Atwater, T., & Stock, J. (1998). Pacific-North America plate tectonics of the Neogene southwestern United States: An update. *International Geology Review*, *40*(5), 375–402. https://doi.org/10.1080/00206819809465216

Axen, G. J., Taylor, W. J., & Bartley, J. M. (1993). Space-time patterns and tectonic controls of Tertiary extension and magmatism in the Great Basin of the western United States. *Geological Society of America Bulletin*, *105*(1), 56–76. https://doi.org/10.1130/0016-7606(1993)105<0056:STPATC>2.3.CO;2

Axen, G. J., Van Wijk, J. W., & Currie, C. A. (2018). Basal continental mantle lithosphere displaced by flat-slab subduction. *Nature Geoscience*, *11*(12), 961–964. https://doi.org/10.1038/s41561-018-0263-9

Bahadori, A., & Holt, W. E. (2019). Geodynamic evolution of southwestern North America since the Late Eocene. *Nature Communications*, *10*(1), 5213. https://doi.org/10.1038/s41467-019-12950-8

Bahadori, A., Holt, W. E., Austermann, J., Campbell, L., Rasbury, E. T., Davis, D. M., et al. (2022). The role of gravitational body forces in the development of metamorphic core complexes. *Nature Communications*, *13*(1), 5646. https://doi.org/10.1038/s41467-022-33361-2

Bahadori, A., Holt, W. E., Feng, R., Austermann, J., Loughney, K. M., Salles, T., et al. (2022). Coupled influence of tectonics, climate, and surface processes on landscape evolution in southwestern North America. *Nature Communications*, *13*(1), 4437. https://doi.org/10.1038/s41467-022-31903-2

Bahadori, A., Holt, W. E., & Rasbury, E. T. (2018). Reconstruction modeling of crustal thickness and paleotopography of western North America since 36 Ma. *Geosphere*, *14*(3), 1207–1231. https://doi.org/10.1130/GES01604.1

Barth, A. P., Wooden, J. L., Jacobson, C. E., & Probst, K. (2004). U-Pb geochronology and geochemistry of the McCoy Mountains Formation, southeastern California: A Cretaceous retroarc foreland basin. *Geological Society of America Bulletin*, *116*(1–2), 142–153. https://doi.org/10.1130/B25288.1

Basler, L. C., & Cassel, E. J. (2025). Surface uplift of the central Cascade Range, northwestern USA, via Oligocene to early Miocene crustal thickening. *Geology*, *53*(10), 864–868. https://doi.org/10.1130/G53421.1

Basler, L., Carrapa, B., Kapp, P., & Ducea, M. N. (2026). Data and results for "Crustal thickness and elevation of the North American Cordillera from the Late Cretaceous to Early Miocene" [Dataset]. *Zenodo*. https://doi.org/10.5281/zenodo.18078382

Beck, S. L., Zandt, G., Myers, S. C., Wallace, T. C., Silver, P. G., & Drake, L. (1996). Crustal-thickness variations in the central Andes. *Geology*, *24*(5), 407–410. https://doi.org/10.1130/0091-7613(1996)024<0407:CTVITC>2.3.CO;2

Best, M. G., Barr, D. L., Christiansen, E. H., Gromme, S., Deino, A. L., & Tingey, D. G. (2009). The Great Basin Altiplano during the middle Cenozoic ignimbrite flareup: Insights from volcanic rocks. *International Geology Review*, *51*(7–8), 589–633. https://doi.org/10.1080/00206810902867690

Best, M. G., & Christiansen, E. H. (1991). Limited extension during peak Tertiary volcanism, Great Basin of Nevada and Utah. *Journal of Geophysical Research*, *96*(B8), 13509–13528. https://doi.org/10.1029/91JB00244

Best, M. G., Christiansen, E. H., De Silva, S., & Lipman, P. W. (2016). Slab-rollback ignimbrite flareups in the southern Great Basin and other Cenozoic American arcs: A distinct style of arc volcanism. *Geosphere*, *12*(4), 1097–1135. https://doi.org/10.1130/GES01285.1

Biek, R. F. (2013). Whole-rock geochemical data for the Panguitch 30′ × 60′ Quadrangle, Iron, Garfield, and Kane Counties. *Utah Geological Survey Open-File Report 623*. Retrieved from https://ugspub.nr.utah.gov/publications/open_file_reports/ofr-623/ofr-623.pdf

Bird, P. (1991). Lateral extrusion of lower crust from under high topography in the isostatic limit. *Journal of Geophysical Research*, *96*(B6), 10275–10286. https://doi.org/10.1029/91JB00370

Blisniuk, P. M., & Stern, L. A. (2005). Stable isotope paleoaltimetry: A critical review. *American Journal of Science*, *305*(10), 1033–1074. https://doi.org/10.2475/ajs.305.10.1033

Block, L., & Royden, L. H. (1990). Core complex geometries and regional scale flow in the lower crust. *Tectonics*, *9*(4), 557–567. https://doi.org/10.1029/TC009i004p00557

Brown, R. L., & Gibson, H. D. (2006). An argument for channel flow in the southern Canadian Cordillera and comparison with Himalayan tectonics. *Geological Society, London, Special Publications*, *268*(1), 543–559. https://doi.org/10.1144/GSL.SP.2006.268.01.25

Buck, W. R. (1991). Modes of continental lithospheric extension. *Journal of Geophysical Research*, *96*(B12), 20161–20178. https://doi.org/10.1029/91JB01485

Butcher, L. A., Mahan, K. H., & Allaz, J. M. (2017). Late Cretaceous crustal hydration in the Colorado Plateau, USA, from xenolith petrology and monazite geochronology. *Lithosphere*, L583.1. https://doi.org/10.1130/L583.1

Byerly, A., Tikoff, B., Kahn, M., Jicha, B., Gaschnig, R., & Fayon, A. K. (2017). Internal fabrics of the Idaho batholith, USA. *Lithosphere*, *9*(2), 283–298. https://doi.org/10.1130/L551.1

Bykerk-Kauffman, A., & Janecke, S. U. (1987). Late Cretaceous to early Tertiary ductile deformation: Catalina-Rincon metamorphic core complex, southeastern Arizona. *Geology*, *15*(5), 462–465. https://doi.org/10.1130/0091-7613(1987)15<462:LCTETD>2.0.CO;2

Camp, V. E., Pierce, K. L., & Morgan, L. A. (2015). Yellowstone plume trigger for Basin and Range extension, and coeval emplacement of the Nevada–Columbia Basin magmatic belt. *Geosphere*, *11*(2), 203–225. https://doi.org/10.1130/GES01051.1

Cassel, E. J., Breecker, D. O., Henry, C. D., Larson, T. E., & Stockli, D. F. (2014). Profile of a paleo-orogen: High topography across the present-day Basin and Range from 40 to 23 Ma. *Geology*, *42*(11), 1007–1010. https://doi.org/10.1130/G35924.1

Cassel, E. J., Smith, M. E., & Jicha, B. R. (2018). The impact of slab rollback on Earth's surface: Uplift and extension in the hinterland of the North American Cordillera. *Geophysical Research Letters*, *45*(20), 10996–11004. https://doi.org/10.1029/2018GL079887

Caylor, E. A., Carrapa, B., Sundell, K., DeCelles, P. G., & Smith, J. M. (2021). Age and deposition of the Fort Crittenden Formation: A window into Late Cretaceous Laramide and Cenozoic tectonics in southeastern Arizona. *Geological Society of America Bulletin*, *133*(9–10), 1996–2016. https://doi.org/10.1130/B35808.1

Chamberlain, C. P., Ibarra, D. E., Kukla, T., Methner, K. A., & Gao, Y. (2021). Triple oxygen isotope paleoaltimetry of crystalline rocks. *Frontiers in Earth Science*, *9*, 633687. https://doi.org/10.3389/feart.2021.633687

Chamberlain, C. P., Mix, H. T., Mulch, A., Hren, M. T., Kent-Corson, M. L., Davis, S. J., et al. (2012). The Cenozoic climatic and topographic evolution of the western North American Cordillera. *American Journal of Science*, *312*(2), 213–262. https://doi.org/10.2475/02.2012.05

Chapman, A., Shields, J., Ducea, M., & Saleeby, J. (2020). Fate of the lower lithosphere during shallow-angle subduction: The Laramide example. *Geological Society of America Today*, *30*(1), 4–10. https://doi.org/10.1130/GSATG412A.1

Chapman, A. D. (2017). The Pelona–Orocopia–Rand and related schists of southern California: A review of the best-known archive of shallow subduction on the planet. *International Geology Review*, *59*(5–6), 664–701. https://doi.org/10.1080/00206814.2016.1230836

Chapman, J. B., Clinkscales, C., Trzinski, A., & Daniel, M. (2025). Evidence for a Late Cretaceous to Paleogene basement-involved retroarc wedge in the southern U.S. Cordillera: A case study from the northern Chiricahua Mountains, Arizona. *Geological Society of America Bulletin*, *137*(3–4), 1827–1842. https://doi.org/10.1130/B37877.1

Chapman, J. B., Ducea, M. N., DeCelles, P. G., & Profeta, L. (2015). Tracking changes in crustal thickness during orogenic evolution with Sr/Y: An example from the North American Cordillera. *Geology*, *43*(10), 919–922. https://doi.org/10.1130/G36996.1

Chapman, J. B., Greig, R., & Haxel, G. B. (2020). Geochemical evidence for an orogenic plateau in the southern U.S. and northern Mexican Cordillera during the Laramide orogeny. *Geology*, *48*(2), 164–168. https://doi.org/10.1130/G47117.1

Chapman, J. B., Pridmore, C., Chamberlain, K., Haxel, G., & Ducea, M. (2023). Himalayan-like crustal melting and differentiation in the southern North American Cordilleran Anatectic Belt during the Laramide Orogeny: Coyote Mountains, Arizona. *Journal of Petrology*, *64*(10), egad075. https://doi.org/10.1093/petrology/egad075

Chapman, J. B., Runyon, S. E., Shields, J. E., Lawler, B. L., Pridmore, C. J., Scoggin, S. H., et al. (2021). The North American Cordilleran anatectic belt. *Earth-Science Reviews*, *215*, 103576. https://doi.org/10.1016/j.earscirev.2021.103576

Chapman, J. B., Scoggin, S. H., Jepson, G., Ricketts, J. W., Schaen, A. J., & Trzinski, A. E. (2024). Oligocene-Miocene exhumation of the Pinaleño metamorphic core complex, Southeastern Arizona: Support for magmatism and plate margin reorganization as controls on regional exhumation trends. *Tectonics*, *43*(4), e2023TC008032. https://doi.org/10.1029/2023TC008032

Chetel, L. M., Janecke, S. U., Carroll, A. R., Beard, B. L., Johnson, C. M., & Singer, B. S. (2011). Paleogeographic reconstruction of the Eocene Idaho River, North American Cordillera. *Geological Society of America Bulletin*, *123*(1–2), 71–88. https://doi.org/10.1130/B30213.1

Chiaradia, M. (2015). Crustal thickness control on Sr/Y signatures of recent arc magmas: An Earth scale perspective. *Scientific Reports*, *5*(1), 8115. https://doi.org/10.1038/srep08115

Christiansen, E. H. (2009). Whole-rock geochemical data for the Soldiers Pass quadrangle, Utah. *Utah Geological Survey Open-File Report 552*. Retrieved from https://ugspub.nr.utah.gov/publications/open_file_reports/ofr-552.pdf

Clark, D. L. (2007). Whole-rock geochemical data for the Skinner Peaks quadrangle, Utah. *Utah Geological Survey Open File Report 494*. https://doi.org/10.34191/OFR-494

Clark, D. L. (2015). Whole-rock geochemical data for Dugway Proving Ground and adjacent areas, Tooele County, Utah. *Utah Geological Survey Open-File Report 645*. Retrieved from https://ugspub.nr.utah.gov/publications/open_file_reports/ofr-645/ofr-645.pdf

Clark, D. L., & Biek, R. F. (2017). Whole-rock geochemical data for the Tooele 30′ × 60′ Quadrangle and the Copperton 7.5' Quadrangle, Utah. *Utah Geological Survey Open-File Report 665*. Retrieved from https://ugspub.nr.utah.gov/publications/open_file_reports/ofr-665/ofr-665.pdf

Colgan, J. P., Dumitru, T. A., Reiners, P. W., Wooden, J. L., & Miller, E. L. (2006). Cenozoic tectonic evolution of the Basin and Range Province in northwestern Nevada. *American Journal of Science*, *306*(8), 616–654. https://doi.org/10.2475/08.2006.02

Colgan, J. P., & Henry, C. D. (2009). Rapid middle Miocene collapse of the Mesozoic orogenic plateau in north-central Nevada. *International Geology Review*, *51*(9–11), 920–961. https://doi.org/10.1080/00206810903056731

Colgan, J. P., Howard, K. A., Fleck, R. J., & Wooden, J. L. (2010). Rapid middle Miocene extension and unroofing of the southern Ruby Mountains, Nevada. *Tectonics*, *29*(6). https://doi.org/10.1029/2009TC002655

Coney, P. J. (1987). The regional tectonic setting and possible causes of Cenozoic extension in the North American Cordillera. *Geological Society, London, Special Publications*, *28*(1), 177–186. https://doi.org/10.1144/GSL.SP.1987.028.01.13

Coney, P. J., & Harms, T. A. (1984). Cordilleran metamorphic core complexes: Cenozoic extensional relics of Mesozoic compression. *Geology*, *12*(9), 550–554. https://doi.org/10.1130/0091-7613(1984)12<550:CMCCCE>2.0.CO;2

Coney, P. J., & Reynolds, S. J. (1977). Cordilleran Benioff zones. *Nature*, *270*(5636), 403–406. https://doi.org/10.1038/270403a0

Constenius, K. N. (1996). Late Paleogene extensional collapse of the Cordilleran foreland fold and thrust belt. *Geological Society of America Bulletin*, *108*(1), 20–39. https://doi.org/10.1130/0016-7606(1996)108<0020:lpecot>2.3.co;2

Coogan, J. C. (1992). *Thrust systems and displacement transfer in the Wyoming-Idaho-Utah thrust belt* (Doctoral dissertation). University of Wyoming. Retrieved from https://www.proquest.com/docview/304001482

Copeland, P., Currie, C. A., Lawton, T. F., & Murphy, M. A. (2017). Location, location, location: The variable lifespan of the Laramide orogeny. *Geology*, *45*(3), 223–226. https://doi.org/10.1130/G38810.1

Davis, G. H. (1979). Laramide folding and faulting in southeastern Arizona. *American Journal of Science*, *279*(5), 543–569. https://doi.org/10.2475/ajs.279.5.543

Davis, S. J., Wiegand, B. A., Carroll, A. R., & Chamberlain, C. P. (2008). The effect of drainage reorganization on paleoaltimetry studies: An example from the Paleogene Laramide foreland. *Earth and Planetary Science Letters*, *275*(3–4), 258–268. https://doi.org/10.1016/j.epsl.2008.08.009

DeCelles, P. G. (2004). Late Jurassic to Eocene evolution of the Cordilleran thrust belt and foreland basin system, western U.S.A. *American Journal of Science*, *304*(2), 105–168. https://doi.org/10.2475/ajs.304.2.105

DeCelles, P. G., & Carrapa, B. (2023). Differences between the central Andean and Himalayan orogenic wedges: A matter of climate. *Earth and Planetary Science Letters*, *616*, 118216. https://doi.org/10.1016/j.epsl.2023.118216

DeCelles, P. G., & Coogan, J. C. (2006). Regional structure and kinematic history of the Sevier fold-and-thrust belt, central Utah. *Geological Society of America Bulletin*, *118*(7–8), 841–864. https://doi.org/10.1130/B25759.1

DeCelles, P. G., Ducea, M. N., Kapp, P., & Zandt, G. (2009). Cyclicity in Cordilleran orogenic systems. *Nature Geoscience*, *2*(4), 251–257. https://doi.org/10.1038/ngeo469

DeCelles, P. G., & Giles, K. A. (1996). Foreland basin systems. *Basin Research*, *8*(2), 105–123. https://doi.org/10.1046/j.1365-2117.1996.01491.x

DeCelles, P. G., & Graham, S. A. (2015). Cyclical processes in the North American Cordilleran orogenic system. *Geology*, *43*(6), 499–502. https://doi.org/10.1130/G36482.1

Dewey, J. F. (1988). Extensional collapse of orogens. *Tectonics*, *7*(6), 1123–1139. https://doi.org/10.1029/TC007i006p01123

Dhuime, B., Wuestefeld, A., & Hawkesworth, C. J. (2015). Emergence of modern continental crust about 3 billion years ago. *Nature Geoscience*, *8*(7), 552–555. https://doi.org/10.1038/ngeo2466

Dickinson, W. R. (2012). Provenance of the Paleogene Colton Formation (Uinta Basin) and Cretaceous–Paleogene provenance evolution in the Utah foreland: Evidence from U-Pb ages of detrital zircons, paleocurrent trends, and sandstone petrofacies. *Geosphere*, *8*(4), 854. https://doi.org/10.1130/GES00763.1

Dickinson, W. R. (1991). *Tectonic setting of faulted Tertiary strata associated with the Catalina core complex in southern Arizona* (Vol. 264). Geological Society of America. https://doi.org/10.1130/SPE264

Dickinson, W. R. (2002). The Basin and Range Province as a composite extensional domain. *International Geology Review*, *44*(1), 1–38. https://doi.org/10.2747/0020-6814.44.1.1

Dickinson, W. R. (2004). Evolution of the North American Cordillera. *Annual Review of Earth and Planetary Sciences*, *32*(1), 13–45. https://doi.org/10.1146/annurev.earth.32.101802.120257

Dickinson, W. R., & Snyder, W. S. (1979). Geometry of subducted slabs related to San Andreas transform. *The Journal of Geology*, *87*(6), 609–627. https://doi.org/10.1086/628456

Dombroski, B. A., & Fodor, R. V. (2019). The Miocene Goldfield-Superstition volcanic province, central Arizona, USA: Geochemically distinct rhyolite sources, 20.5 to 19 Ma. *Lithos*, *330–331*, 139–159. https://doi.org/10.1016/j.lithos.2019.02.008

Du Bray, E., & John, D. (2011). Petrologic, tectonic, and metallogenic evolution of the Ancestral Cascades magmatic arc, Washington, Oregon, and northern California. *Geosphere*, *7*(5), 1102–1133. https://doi.org/10.1130/GES00669.1

Ducea, M. N., & Barton, M. D. (2007). Igniting flare-up events in Cordilleran arcs. *Geology*, *35*(11), 1047. https://doi.org/10.1130/g23898a.1

Ducea, M. N., Chapman, A. D., Bowman, E., & Balica, C. (2021). Arclogites and their role in continental evolution; part 2: Relationship to batholiths and volcanoes, density and foundering, remelting and long-term storage in the mantle. *Earth-Science Reviews*, *214*, 103476. https://doi.org/10.1016/j.earscirev.2020.103476

Ducea, M. N., Chapman, A. D., Bowman, E., & Triantafyllou, A. (2021). Arclogites and their role in continental evolution; part 1: Background, locations, petrography, geochemistry, chronology and thermobarometry. *Earth-Science Reviews*, *214*, 103375. https://doi.org/10.1016/j.earscirev.2020.103375

Ducea, M. N., & Saleeby, J. B. (1998). A case for delamination of the deep batholithic crust beneath the Sierra Nevada, California. *International Geology Review*, *40*(1), 78–93. https://doi.org/10.1080/00206819809465199

Ducea, M. N., Saleeby, J. B., & Bergantz, G. (2015). The architecture, chemistry, and evolution of continental magmatic arcs. *Annual Review of Earth and Planetary Sciences*, *43*(1), 299–331. https://doi.org/10.1146/annurev-earth-060614-105049

Dudás, F. Ö., Ispolatov, V. O., Harlan, S. S., & Snee, L. W. (2010). $^{40}Ar/^{39}Ar$ geochronology and geochemical reconnaissance of the Eocene Lowland Creek volcanic field, west-central Montana. *The Journal of Geology*, *118*(3), 295–304. https://doi.org/10.1086/651523

Erdman, M. E., Lee, C.-T. A., Levander, A., & Jiang, H. (2016). Role of arc magmatism and lower crustal foundering in controlling elevation history of the Nevadaplano and Colorado Plateau: A case study of pyroxenitic lower crust from central Arizona, USA. *Earth and Planetary Science Letters*, *439*, 48–57. https://doi.org/10.1016/j.epsl.2016.01.032

Evans, S. L., Styron, R. H., Van Soest, M. C., Hodges, K. V., & Hanson, A. D. (2015). Zircon and apatite (U-Th)/He evidence for Paleogene and Neogene extension in the Southern Snake Range, Nevada, USA: South Snake Range extension. *Tectonics*, *34*(10), 2142–2164. https://doi.org/10.1002/2015TC003913

Fan, M., Constenius, K. N., & Dettman, D. L. (2017). Prolonged high relief in the northern Cordilleran orogenic front during middle and late Eocene extension based on stable isotope paleoaltimetry. *Earth and Planetary Science Letters*, *457*, 376–384. https://doi.org/10.1016/j.epsl.2016.10.038

Farmer, G. L., Bailley, T., & Elkins-Tanton, L. T. (2008). Mantle source volumes and the origin of the mid-Tertiary ignimbrite flare-up in the southern Rocky Mountains, western U.S. *Lithos*, *102*(1–2), 279–294. https://doi.org/10.1016/j.lithos.2007.08.014

Farner, M. J., & Lee, C.-T. A. (2017). Effects of crustal thickness on magmatic differentiation in subduction zone volcanism: A global study. *Earth and Planetary Science Letters*, *470*, 96–107. https://doi.org/10.1016/j.epsl.2017.04.025

Favorito, D. A., & Seedorff, E. (2021). Cenozoic structural evolution of the Catalina metamorphic core complex and reassembly of Laramide reverse faults, southeastern Arizona, USA. *Geosphere*, *17*(6), 1928–1971. https://doi.org/10.1130/GES02313.1

Fayon, A. K., Peacock, S. M., Stump, E., & Reynolds, S. J. (2000). Fission track analysis of the footwall of the Catalina detachment fault, Arizona: Tectonic denudation, magmatism, and erosion. *Journal of Geophysical Research*, *105*(B5), 11047–11062. https://doi.org/10.1029/1999JB900421

Feeley, T. C., & Grunder, A. L. (1991). Mantle contribution to the evolution of Middle Tertiary silicic magmatism during early stages of extension: The Egan Range volcanic complex, east-central Nevada. *Contributions to Mineralogy and Petrology*, *106*(2), 154–169. https://doi.org/10.1007/BF00306431

Feng, R., Poulsen, C. J., Werner, M., Chamberlain, C. P., Mix, H. T., & Mulch, A. (2013). Early Cenozoic evolution of topography, climate, and stable isotopes in precipitation in the North American Cordillera. *American Journal of Science*, *313*(7), 613–648. https://doi.org/10.2475/07.2013.01

Foreman, B. Z., Fricke, H. C., Lohmann, K. C., & Rogers, R. R. (2011). Reconstructing paleocatchments by integrating stable isotope records, sedimentology, and taphonomy: A late Cretaceous case study (Montana, United States). *PALAIOS*, *26*(9), 545–554. https://doi.org/10.2110/palo.2010.p10-133r

Fricke, H. C., Foreman, B. Z., & Sewall, J. O. (2010). Integrated climate model-oxygen isotope evidence for a North American monsoon during the Late Cretaceous. *Earth and Planetary Science Letters*, *289*(1–2), 11–21. https://doi.org/10.1016/j.epsl.2009.10.018

Fuentes, F. (2012). Regional structure and kinematic history of the Cordilleran fold-thrust belt in northwestern Montana, USA. *Geosphere*, *8*(5), 1104–1128. https://doi.org/10.1130/GES00773.1

Galewsky, J. (2009). Orographic precipitation isotopic ratios in stratified atmospheric flows: Implications for paleoelevation studies. *Geology*, *37*(9), 791–794. https://doi.org/10.1130/G30008A.1

Gans, P. B. (1987). An open-system, two-layer crustal stretching model for the eastern Great Basin. *Tectonics*, *6*(1), 1–12. https://doi.org/10.1029/TC006i001p00001

Gans, P. B., Mahood, G. A., & Schermer, E. (1989). Synextensional magmatism in the Basin and Range Province; A case study from the eastern Great Basin. In *Geological society of America special papers* (Vol. 233, pp. 1–53). Geological Society of America. https://doi.org/10.1130/SPE233-p1

Garzione, C. N., Hoke, G. D., Libarkin, J. C., Withers, S., MacFadden, B., Eiler, J., et al. (2008). Rise of the Andes. *Science*, *320*(5881), 1304–1307. https://doi.org/10.1126/science.1148615

Garzione, C. N., McQuarrie, N., Perez, N. D., Ehlers, T. A., Beck, S. L., Kar, N., et al. (2017). Tectonic evolution of the central Andean Plateau and implications for the growth of plateaus. *Annual Review of Earth and Planetary Sciences*, *45*(1), 529–559. https://doi.org/10.1146/annurev-earth-063016-020612

Gaschnig, R. M., Vervoort, J. D., Lewis, R. S., & Tikoff, B. (2011). Isotopic evolution of the Idaho Batholith and Challis Intrusive Province, northern U.S. Cordillera. *Journal of Petrology*, *52*(12), 2397–2429. https://doi.org/10.1093/petrology/egr050

Gehrels, G. E., & Smith, C. H. (1991). U-Pb geochronologic constraints on the age of thrusting, crustal extension, and peraluminous plutonism in the Little Rincon Mountains, southern Arizona. *Geology*, *19*(3), 238–241. https://doi.org/10.1130/0091-7613(1991)019<0238:UPGCOT>2.3.CO;2

Glazner, A. F. (2022). Cenozoic magmatism and plate tectonics in western North America: Have we got it wrong? In G. R. Foulger, L. C. Hamilton, D. M. Jurdy, C. A. Stein, K. A. Howard, & S. Stein (Eds.), *In the footsteps of Warren B. Hamilton: New ideas in Earth science* (pp. 95–108). Geological Society of America. https://doi.org/10.1130/2021.2553(09)

Gottardi, R., McAleer, R., Casale, G., Borel, M., Iriondo, A., & Jepson, G. (2020). Exhumation of the Coyote Mountains metamorphic core complex (Arizona): Implications for orogenic collapse of the southern North American Cordillera. *Tectonics*, *39*(8), e2019TC006050. https://doi.org/10.1029/2019TC006050

Hammond, P. (1979). A tectonic model for evolution of the Cascade Range. In J. M. Armentrout, M. R. Cole, & H. TerBest (Eds.), *Pacific Coast paleogeography symposium 3: Cenozoic paleogeography of the Western U.S* (pp. 219–237). Pacific Section SEPM.

Henry, C. D. (2008). Ash-flow tuffs and paleovalleys in northeastern Nevada: Implications for Eocene paleogeography and extension in the Sevier hinterland, northern Great Basin. *Geosphere*, *4*(1), 1–35. https://doi.org/10.1130/GES00122.1

Henry, C. D., Hinz, N. H., Faulds, J. E., Colgan, J. P., John, D. A., Brooks, E. R., et al. (2012). Eocene-Early Miocene paleotopography of the Sierra Nevada-Great Basin-Nevadaplano based on widespread ash-flow tuffs and paleovalleys. *Geosphere*, *8*(1), 1–27. https://doi.org/10.1130/GES00727.1

Henry, C. D., McGrew, A. J., Colgan, J. P., Snoke, A. W., & Brueseke, M. E. (2011). Timing, distribution, amount, and style of Cenozoic extension in the northern Great Basin. In *Geologic field trips to the basin and range, Rocky Mountains, Snake River Plain, and Terranes of the U.S. Cordillera* (pp. 27–66). Geological Society of America. https://doi.org/10.1130/2011.0021(02)

Hildreth, W., & Moorbath, S. (1988). Crustal contributions to arc magmatism in the Andes of central Chile. *Contributions to Mineralogy and Petrology*, *98*(4), 455–489. https://doi.org/10.1007/BF00372365

Hiza. (1999). *The geochemistry and geochronology of the Eocene Absaroka volcanic province, northern Wyoming and southwest Montana, United States of America* (Doctoral dissertation). Oregon State University. Retrieved from https://www.proquest.com/docview/304536899

Hodges, K. V., & Walker, J. D. (1992). Extension in the Cretaceous Sevier orogen, North American Cordillera. *Geological Society of America Bulletin*, *104*(5), 560. https://doi.org/10.1130/0016-7606(1992)104<0560:EITCSO>2.3.CO;2

Horton, T. W. (2004). Spatial and temporal variation of Cenozoic surface elevation in the Great Basin and Sierra Nevada. *American Journal of Science*, *304*(10), 862–888. https://doi.org/10.2475/ajs.304.10.862

Howlett, C. J., Reynolds, A. N., & Laskowski, A. K. (2021). Magmatism and extension in the Anaconda metamorphic core complex of western Montana and relation to regional tectonics. *Tectonics*, *40*(9), e2020TC006431. https://doi.org/10.1029/2020TC006431

Humphreys, E. (2009). Relation of flat subduction to magmatism and deformation in the western United States. In S. M. Kay, V. A. Ramos, & W. R. Dickinson (Eds.), *Backbone of the Americas: Shallow subduction, plateau uplift, and ridge and terrane collision* (pp. 85–98). Geological Society of America. https://doi.org/10.1130/2009.1204(04)

Humphreys, E. D., Hessler, E., Dueker, K., Farmer, G. L., Erslev, E., & Atwater, T. (2003). How Laramide-Age Hydration of North American Lithosphere by the Farallon Slab Controlled Subsequent Activity in the Western United States. *International Geology Review*, *45*(7), 575–595. https://doi.org/10.2747/0020-6814.45.7.575

Humphreys, E. D. (1995). Post-Laramide removal of the Farallon slab, western United States. *Geology*, *23*(11), 987. https://doi.org/10.1130/0091-7613(1995)023<0987:plrotf>2.3.co;2

Humphreys, E. D., & Grunder, A. L. (2022). Tectonic controls on the origin and segmentation of the Cascade Arc, USA. *Bulletin of Volcanology*, *84*(12), 102. https://doi.org/10.1007/s00445-022-01611-2

Ibarra, D. E., Kukla, T., Methner, K. A., Mulch, A., & Chamberlain, C. P. (2021). Reconstructing past elevations from triple oxygen isotopes of lacustrine chert: Application to the Eocene Nevadaplano, Elko Basin, Nevada, United States. *Frontiers in Earth Science*, *9*, 628868. https://doi.org/10.3389/feart.2021.628868

Janecke, S. U. (1994). Sedimentation and paleogeography of an Eocene to Oligocene rift zone, Idaho and Montana. *Geological Society of America Bulletin*, *106*(8), 1083–1095. https://doi.org/10.1130/0016-7606(1994)106<1083:sapoae>2.3.co;2

Janecke, S. U., VanDenburg, C. J., Blankenau, J. J., & M'Gonigle, J. W. (2000). Long-distance longitudinal transport of gravel across the Cordilleran thrust belt of Montana and Idaho. *Geology*, *28*(5), 439. https://doi.org/10.1130/0091-7613(2000)28<439:LLTOGA>2.0.CO;2

Jepson, G., Carrapa, B., George, S. W. M., Reeher, L. J., Kapp, P. A., Davis, G. H., et al. (2022). Where did the Arizona-Plano go? Protracted thinning via upper- to lower-crustal processes. *Journal of Geophysical Research: Solid Earth*, *127*(4), e2021JB023850. https://doi.org/10.1029/2021JB023850

Jepson, G., Carrapa, B., Reeher, L. J., DeCelles, P. G., Afonso, W. D., Howlett, C. J., et al. (2025). Regional exhumation of the Laramide Province. *Geological Society of America Bulletin*, *137*(7–8), 2913–2932. https://doi.org/10.1130/B37625.1

Johnson, C. M. (1991). Large-scale crust formation and lithosphere modification beneath Middle to Late Cenozoic calderas and volcanic fields, western North America. *Journal of Geophysical Research*, *96*(B8), 13485–13507. https://doi.org/10.1029/91JB00304

Jones, C. H. (2025). Late Cretaceous dynamics of the "Mojave Waistland," California, USA. In S. M. Gordon, R. B. Miller, M. E. Rusmore, & B. Tikoff (Eds.), *Jurassic–Paleogene tectonic evolution of the north American Cordillera*. Geological Society of America. https://doi.org/10.1130/2025.2565(16)

Jones, C. H., Farmer, G. L., Sageman, B., & Zhong, S. (2011). Hydrodynamic mechanism for the Laramide orogeny. *Geosphere*, *7*(1), 183–201. https://doi.org/10.1130/GES00575.1

Jones, C. H., Mahan, K. H., Butcher, L. A., Levandowski, W. B., & Farmer, G. L. (2015). Continental uplift through crustal hydration. *Geology*, *43*(4), 355–358. https://doi.org/10.1130/G36509.1

Jones, C. H., Sonder, L. J., & Unruh, J. R. (1998). Lithospheric gravitational potential energy and past orogenesis: Implications for conditions of initial Basin and Range and Laramide deformation. *Geology*, *26*(7), 639. https://doi.org/10.1130/0091-7613(1998)026<0639:LGPEAP>2.3.CO;2

Jordan, B. T. (1994). *Emplacement and exhumation of the southeastern Atlanta Lobe of the Idaho Batholith and outlying stocks, south-central Idaho* (Master's thesis). Idaho State University. Retrieved from https://isu.app.box.com/v/Jordan-1994

Jutzeler, M., McPhie, J., & Allen, S. R. (2014). Facies architecture of a continental, below-wave-base volcaniclastic basin: The Ohanapecosh Formation, Ancestral Cascades arc (Washington, USA). *Geological Society of America Bulletin*, *126*(3–4), 352–376. https://doi.org/10.1130/B30763.1

Kapp, P., Jepson, G., Carrapa, B., Schaen, A. J., He, J. J. Y., & Wang, J. W. (2023). Laramide bulldozing of lithosphere beneath the Arizona transition zone, southwestern United States. *Geology*, *51*(10), 952–956. https://doi.org/10.1130/G51194.1

Kapp, P., Taylor, M., Stockli, D., & Ding, L. (2008). Development of active low-angle normal fault systems during orogenic collapse: Insight from Tibet. *Geology*, *36*(1), 7. https://doi.org/10.1130/G24054A.1

Kent-Corson, M. L., Barnosky, A. D., Mulch, A., Carrasco, M. A., & Chamberlain, C. P. (2013). Possible regional tectonic controls on mammalian evolution in western North America. *Palaeogeography, Palaeoclimatology, Palaeoecology*, *387*, 17–26. https://doi.org/10.1016/j.palaeo.2013.07.014

Kendrick, J., & Yakymchuk, C. (2020). Garnet fractionation, progressive melt loss and bulk composition variations in anatectic metabasites: Complications for interpreting the geodynamic significance of TTGs. *Geoscience Frontiers*, *11*(3), 745–763. https://doi.org/10.1016/j.gsf.2019.12.001

Kent-Corson, M. L., Sherman, L. S., Mulch, A., & Chamberlain, C. P. (2006). Cenozoic topographic and climatic response to changing tectonic boundary conditions in western North America. *Earth and Planetary Science Letters*, *252*(3–4), 453–466. https://doi.org/10.1016/j.epsl.2006.09.049

Knapp, J. H., & Heizler, M. T. (1990). Thermal history of crystalline nappes of the Maria Fold and Thrust Belt, west central Arizona. *Journal of Geophysical Research*, *95*(B12), 20049–20073. https://doi.org/10.1029/JB095iB12p20049

Konstantinou, A. (2022). The "death" of the Sevier-Laramide orogen: Gravitational collapse of the crust or something else? In J. P. Craddock, D. H. Malone, B. Z. Foreman, & A. Konstantinou (Eds.), *Tectonic evolution of the Sevier-Laramide Hinterland, Thrust Belt, and Foreland, and Postorogenic Slab Rollback (180–20 Ma)* (pp. 379–412). Geological Society of America. https://doi.org/10.1130/2021.2555(15)

Lageson, D. R., Kalakay, T. J., & Foster, D. A. (2020). *Mountain building: The orogenic evolution of Montana (No. Montana Bureau of Mines and Geology Special Publication 122). Butte, MT*. Montana Bureau of Mines and Geology.

Lageson, D. R., Schmitt, J. G., Horton, B. K., Kalakay, T. J., & Burton, B. R. (2001). Influence of Late Cretaceous magmatism on the Sevier orogenic wedge, western Montana. *Geology*, *29*(8), 723. https://doi.org/10.1130/0091-7613(2001)029<0723:IOLCMO>2.0.CO;2

Laske, G., Masters, G., Ma, Z., & Pasyanos, M. (2013). Update on CRUST1.0—A 1-degree global model of Earth's crust. In *Geophysical research abstracts* (Vol. 15). Retrieved from https://ui.adsabs.harvard.edu/abs/2013EGUGA..15.2658L

Lechler, A. R., & Niemi, N. A. (2011). Controls on the spatial variability of modern meteoric ^{18}O: Empirical constraints from the western U.S. and East Asia and implications for stable isotope studies. *American Journal of Science*, *311*(8), 664–700. https://doi.org/10.2475/08.2011.02

Lee, C.-T. A., Thurner, S., Paterson, S., & Cao, W. (2015). The rise and fall of continental arcs: Interplays between magmatism, uplift, weathering, and climate. *Earth and Planetary Science Letters*, *425*, 105–119. https://doi.org/10.1016/j.epsl.2015.05.045

Lee, J., Blackburn, T., & Johnston, S. (2017). Timing of mid-crustal ductile extension in the northern Snake Range metamorphic core complex, Nevada: Evidence from U/Pb zircon ages. *Geosphere*, *13*(2), 439–459. https://doi.org/10.1130/GES01429.1

Levy, D. A., Zuza, A. V., Michels, Z. D., & DesOrmeau, J. W. (2023). Buoyant doming generates metamorphic core complexes in the North American Cordillera. *Geology*, *51*(3), 290–294. https://doi.org/10.1130/G50752.1

Li, G., Bidgoli, T. S., Chen, M., Ma, X., & Li, J. (2022). Sedimentary and crustal structure of the western United States from joint inversion of multiple passive seismic datasets. *Journal of Geophysical Research: Solid Earth*, *127*(2), e2021JB022384. https://doi.org/10.1029/2021JB022384

Li, L., DeCelles, P., Kapp, P., Garzione, C., Quade, J., & Yanay, N. (2024). Constraining carbonate diagenesis using clumped isotope temperatures and U-Pb dating: A case study and implications for paleoelevation interpretations in western central Tibet. *Geochimica et Cosmochimica Acta*, *374*, 1–14. https://doi.org/10.1016/j.gca.2024.04.007

Licht, A., Quade, J., Kowler, A., De Los Santos, M., Hudson, A., Schauer, A., et al. (2017). Impact of the North American monsoon on isotope paleoaltimeters: Implications for the paleoaltimetry of the American southwest. *American Journal of Science*, *317*(1), 1–33. https://doi.org/10.2475/01.2017.01

Lieu, W. K., & Stern, R. J. (2019). The robustness of Sr/Y and La/Yb as proxies for crust thickness in modern arcs. *Geosphere*, *15*(3), 621–641. https://doi.org/10.1130/GES01667.1

Lipman, P. W. (2021). Raising the West: Mid-cenozoic Colorado-plano related to subvolcanic batholith assembly in the Southern Rocky Mountains (USA)? *Geology*, *49*(9), 1107–1111. https://doi.org/10.1130/G48963.1

Lipman, P. W., Prostka, H. J., & Christiansen, R. L. (1972). Cenozoic volcanism and plate-tectonic evolution of the western United States. I. Early and Middle Cenozoic. *Philosophical Transactions of the Royal Society of London. Series A, Mathematical and Physical Sciences*, *271*(1213), 217–248. https://doi.org/10.1098/rsta.1972.0008

Liu, B., Williams, S., Seton, M., & Zhao, G. (2024). Mapping paleoelevations along active continental margins with igneous geochemistry: A case study from South America. *Gondwana Research*, *134*, 285–297. https://doi.org/10.1016/j.gr.2024.07.010

Long, S. P. (2019). Geometry and magnitude of extension in the Basin and Range Province (39°N), Utah, Nevada, and California, USA: Constraints from a province-scale cross section. *Geological Society of America Bulletin*, *131*(1–2), 99–119. https://doi.org/10.1130/B31974.1

Long, S. P. (2023). Westward underthrusting of thick North American crust: The dominant thickening process that built the Cordilleran orogenic plateau. *Geology*, *51*(12), 1111–1116. https://doi.org/10.1130/G51339.1

Long, S. P., & Kohn, M. J. (2020). Distributed ductile thinning during thrust emplacement: A commonly overlooked exhumation mechanism. *Geology*, *48*(4), 368–373. https://doi.org/10.1130/G47022.1

Long, S. P., Thomson, S. N., Reiners, P. W., & Di Fiori, R. V. (2015). Synorogenic extension localized by upper-crustal thickening: An example from the Late Cretaceous Nevadaplano. *Geology*, *43*(4), 351–354. https://doi.org/10.1130/G36431.1

Long, S. P., & Walker, J. P. (2015). Geometry and kinematics of the Grant Range brittle detachment system, eastern Nevada, U.S.A.: An end-member style of upper crustal extension. *Tectonics*, *34*(9), 1837–1862. https://doi.org/10.1002/2015TC003918

Luffi, P., & Ducea, M. N. (2022). Chemical Mohometry: Assessing crustal thickness of ancient orogens using geochemical and isotopic data. *Reviews of Geophysics*, *60*(2), e2021RG000753. https://doi.org/10.1029/2021RG000753

Lund Snee, J.-E., & Miller, E. L. (2022). Magmatism, migrating topography, and the transition from Sevier shortening to Basin and Range extension, western United States. In J. P. Craddock, D. H. Malone, B. Z. Foreman, & A. Konstantinou (Eds.), *Tectonic evolution of the Sevier-*

Laramide Hinterland, Thrust Belt, and Foreland, and Postorogenic Slab Rollback (180–20 Ma) (pp. 335–357). Geological Society of America. https://doi.org/10.1130/2021.2555(13)

Mantle, G. W., & Collins, W. J. (2008). Quantifying crustal thickness variations in evolving orogens: Correlation between arc basalt composition and Moho depth. *Geology*, *36*(1), 87. https://doi.org/10.1130/G24095A.1

McKean, A. (2017). Whole-rock geochemical data for the Salt Lake City North, Sugar House, and Draper quadrangles, Utah. *Utah Geological Survey Open-File Report 663*. https://doi.org/10.34191/OFR-663

McKean, A., Christiansen, E., Allen, T., & Kowallis, B. (2013). Whole-rock geochemical data for the Allens Ranch, Boulter Peak, and Goshen quadrangles, Utah. *Utah Geological Survey Open-File Report 617*. https://doi.org/10.34191/OFR-617

McQuarrie, N., & Chase, C. G. (2000). Raising the Colorado Plateau. *Geology*, *28*(1), 91. https://doi.org/10.1130/0091-7613(2000)028<0091:RTCP>2.0.CO;2

McQuarrie, N., & Oskin, M. (2010). Palinspastic restoration of NAVDat and implications for the origin of magmatism in southwestern North America. *Journal of Geophysical Research*, *115*(B10), 2009JB006435. https://doi.org/10.1029/2009JB006435

Methner, K., Fiebig, J., Wacker, U., Umhoefer, P., Chamberlain, C. P., & Mulch, A. (2016). Eocene-Oligocene proto-Cascades topography revealed by clumped (Δ_{47}) and oxygen isotope (δ^{18}O) geochemistry (Chumstick Basin, WA, USA). *Tectonics*, *35*(3), 546–564. https://doi.org/10.1002/2015TC003984

Miller, C. F., & Bradfish, L. J. (1980). An inner Cordilleran belt of muscovite-bearing plutons. *Geology*, *8*(9), 412–416. https://doi.org/10.1130/0091-7613(1980)8<412:AICBOM>2.0.CO;2

Miller, E. L., Dumitru, T. A., Brown, R. W., & Gans, P. B. (1999). Rapid Miocene slip on the Snake Range–Deep Creek Range fault system, east-central Nevada. *Geological Society of America Bulletin*, *111*(6), 886–905. https://doi.org/10.1130/0016-7606(1999)111<0886:RMSOTS>2.3.CO;2

Mix, H. T., Mulch, A., Kent-Corson, M. L., & Chamberlain, C. P. (2011). Cenozoic migration of topography in the North American Cordillera. *Geology*, *39*(1), 87–90. https://doi.org/10.1130/G31450.1

Molnar, P., & Lyon-Caen, H. (1988). Some simple physical aspects of the support, structure, and evolution of mountain belts. In S. P. Clark, B. C. Burchfiel, & J. Suppe (Eds.), *Processes in continental lithospheric deformation* (pp. 179–208). Geological Society of America. https://doi.org/10.1130/SPE218-p179

Mulch, A., Teyssier, C., Cosca, M. A., & Chamberlain, C. P. (2007). Stable isotope paleoaltimetry of Eocene core complexes in the North American Cordillera. *Tectonics*, *26*(4), 1–13. https://doi.org/10.1029/2006TC001995

Nelson, S. T., Davidson, J. P., Friedman, J. D., & Huffman, A. C. (1998). The petrogenesis of the Colorado Plateau laccoliths and their relationship to regional magmatism. In *Laccolithic complexes of southeastern Utah: Time of emplacement and tectonic setting—Workshop proceedings* (Vol. 2158, pp. 85–100). U.S. Geological Survey. Retrieved from https://www.researchgate.net/profile/Stephen-Nelson-2/publication/265578432_The_Petrogenesis_of_the_Colorado_Plateau_Laccoliths_and_Their_Relationship_to_Regional_Magmatism/links/586fce3e08ae329d62162886/The-Petrogenesis-of-the-Colorado-Plateau-Laccoliths-and-Their-Relationship-to-Regional-Magmatism.pdf

Painter, C. S., Carrapa, B., DeCelles, P. G., Gehrels, G. E., & Thomson, S. N. (2014). Exhumation of the North American Cordillera revealed by multi-dating of Upper Jurassic–Upper Cretaceous foreland basin deposits. *Geological Society of America Bulletin*, *126*(11–12), 1439–1464. https://doi.org/10.1130/B30999.1

Pourteau, A., Doucet, L. S., Blereau, E. R., Volante, S., Johnson, T. E., Collins, W. J., et al. (2020). TTG generation by fluid-fluxed crustal melting: Direct evidence from the Proterozoic Georgetown Inlier, NE Australia. *Earth and Planetary Science Letters*, *550*, 116548. https://doi.org/10.1016/j.epsl.2020.116548

Price, R. A. (1981). The Cordilleran foreland thrust and fold belt in the southern Canadian Rocky Mountains. *Geological Society, London, Special Publications*, *9*(1), 427–448. https://doi.org/10.1144/GSL.SP.1981.009.01.39

Priest, G. R. (1990). Volcanic and tectonic evolution of the Cascade Volcanic Arc, central Oregon. *Journal of Geophysical Research*, *95*(B12), 19583–19599. https://doi.org/10.1029/JB095iB12p19583

Profeta, L., Ducea, M. N., Chapman, J. B., Paterson, S. R., Gonzales, S. M. H., Kirsch, M., et al. (2015). Quantifying crustal thickness over time in magmatic arcs. *Scientific Reports*, *5*(1), 17786. https://doi.org/10.1038/srep17786

Quade, J., Leary, R., Dettinger, M. P., Orme, D., Krupa, A., DeCelles, P. G., et al. (2020). Resetting Southern Tibet: The serious challenge of obtaining primary records of paleoaltimetry. *Global and Planetary Change*, *191*, 103194. https://doi.org/10.1016/j.gloplacha.2020.103194

Rautela, O., Chapman, A. D., Shields, J. E., Ducea, M. N., Lee, C.-T., Jiang, H., & Saleeby, J. (2020). In search for the missing arc root of the Southern California Batholith: P-t-t evolution of upper mantle xenoliths of the Colorado Plateau Transition Zone. *Earth and Planetary Science Letters*, *547*, 116447. https://doi.org/10.1016/j.epsl.2020.116447

Roberts, N. M. W., Hernández-Montenegro, J. D., & Palin, R. M. (2024). Garnet stability during crustal melting: Implications for chemical mohometry and secular change in arc magmatism and continent formation. *Chemical Geology*, *659*, 122142. https://doi.org/10.1016/j.chemgeo.2024.122142

Rowley, D. B. (2007). Stable isotope-based paleoaltimetry: Theory and validation. *Reviews in Mineralogy and Geochemistry*, *66*(1), 23–52. https://doi.org/10.2138/rmg.2007.66.2

Rowley, D. B., Pierrehumbert, R. T., & Currie, B. S. (2001). A new approach to stable isotope-based paleoaltimetry: Implications for paleoaltimetry and paleohypsometry of the High Himalaya since the Late Miocene. *Earth and Planetary Science Letters*, *188*(1–2), 253–268. https://doi.org/10.1016/S0012-821X(01)00324-7

Roy, M., Jordan, T. H., & Pederson, J. (2009). Colorado Plateau magmatism and uplift by warming of heterogeneous lithosphere. *Nature*, *459*(7249), 978–982. https://doi.org/10.1038/nature08052

Salem, A. C. (2009). *Mesozoic tectonics of the Maria fold and thrust belt and McCoy basin: An examination of polyphase deformation and synorogenic response* (M.S. Thesis). University of New Mexico. Retrieved from https://digitalrepository.unm.edu/eps_etds/75/

Scarberry, K. C., Yakovlev, P. V., & Schwartz, T. M. (2021). *Mesozoic magmatism in Montana (No. Montana Bureau of Mines and Geology Special Publication 122)* (pp. 1–30). Montana Bureau of Mines and Geology.

Schellart, W. P., & Strak, V. (2021). Geodynamic models of short-lived, long-lived and periodic flat slab subduction. *Geophysical Journal International*, *226*(3), 1517–1541. https://doi.org/10.1093/gji/ggab126

Schmandt, B., & Humphreys, E. (2011). Seismically imaged relict slab from the 55 Ma Siletzia accretion to the northwest United States. *Geology*, *39*(2), 175–178. https://doi.org/10.1130/G31558.1

Schwartz, T. M., Methner, K., Mulch, A., Graham, S. A., & Chamberlain, C. P. (2019). Paleogene topographic and climatic evolution of the Northern Rocky Mountains from integrated sedimentary and isotopic data. *Geological Society of America Bulletin*, *131*(7–8), 1203–1223. https://doi.org/10.1130/B32068.1

Schwartz, T. M., & Schwartz, R. K. (2013). Paleogene postcompressional intermontane basin evolution along the frontal Cordilleran fold-and-thrust belt of southwestern Montana. *Geological Society of America Bulletin*, *125*(5–6), 961–984. https://doi.org/10.1130/B30766.1

Sewall, J. O., & Sloan, L. C. (2006). Come a little bit closer: A high-resolution climate study of the early Paleogene Laramide foreland. *Geology*, *34*(2), 81–84. https://doi.org/10.1130/G22177.1

Seymour, N. M., Strickland, E. D., Singleton, J. S., Stockli, D. F., & Wong, M. S. (2018). Laramide subduction and metamorphism of the Orocopia Schist, northern Plomosa Mountains, west-central Arizona: Insights from zircon U-Pb geochronology. *Geology*, *46*(10), 847–850. https://doi.org/10.1130/G45059.1

Sharman, G. R., Covault, J. A., Stockli, D. F., Wroblewski, A. F.-J., & Bush, M. A. (2017). Early Cenozoic drainage reorganization of the United States Western Interior–Gulf of Mexico sediment routing system. *Geology*, *45*(2), 187–190. https://doi.org/10.1130/G38765.1

Shen, W., & Ritzwoller, M. H. (2016). Crustal and uppermost mantle structure beneath the United States. *Journal of Geophysical Research: Solid Earth*, *121*(6), 4306–4342. https://doi.org/10.1002/2016JB012887

Singleton, J. S. (2013). Development of extension-parallel corrugations in the Buckskin-Rawhide metamorphic core complex, west-central Arizona. *Geological Society of America Bulletin*, *125*(3–4), 453–472. https://doi.org/10.1130/B30672.1

Smiley, T. M., Bahadori, A., Rasbury, E. T., Holt, W. E., & Badgley, C. (2024). Tectonic extension and paleoelevation influence mammalian diversity dynamics in the Basin and Range Province of western North America. *Science Advances*, *10*(25), eadn6842. https://doi.org/10.1126/sciadv.adn6842

Smith, M. E., Cassel, E. J., Jicha, B. R., Singer, B. S., & Canada, A. S. (2017). Hinterland drainage closure and lake formation in response to middle Eocene Farallon slab removal, Nevada, U.S.A. *Earth and Planetary Science Letters*, *479*, 156–169. https://doi.org/10.1016/j.epsl.2017.09.023

Sonder, L. J., & Jones, C. H. (1999). Western United States extension: How the West was widened. *Annual Review of Earth and Planetary Sciences*, *27*(1), 417–462. https://doi.org/10.1146/annurev.earth.27.1.417

Spencer, J. E., & Reynolds, S. J. (1990). Relationship between Mesozoic and Cenozoic tectonic features in west central Arizona and adjacent southeastern California. *Journal of Geophysical Research*, *95*(B1), 539–555. https://doi.org/10.1029/JB095iB01p00539

Spencer, J. E., Richard, S. M., Bykerk-Kauffman, A., Constenius, K. N., & Valencia, V. A. (2022). Structure, chronology, kinematics, and geodynamics of tectonic extension in the greater Catalina metamorphic core complex, southeastern Arizona, USA. *Geosphere*, *18*(6), 1643–1678. https://doi.org/10.1130/GES02485.1

Sundell, K., Laskowski, A., Kapp, P., Ducea, M., & Chapman, J. (2021). Jurassic to Neogene quantitative crustal thickness estimates in southern Tibet. *Geological Society of America Today*, *31*(6), 4–10. https://doi.org/10.1130/GSATG461A.1

Tepper, J. H., & Clark, K. P. (2024). Initiation of the Cascade arc. *Geology*, *52*(4), 297–301. https://doi.org/10.1130/G51888.1

Tepper, J. H., Loewen, M. W., Caulfield, L. M., Davidson, P. C., Ruthenberg, K. L., Blakely, S. W. F., et al. (2023). Petrology and geochronology of Cretaceous−Eocene plutonic rocks in northeastern Washington, USA: Crustal thickening, slab rollback, and origin of the Challis episode. *Geological Society of America Bulletin*, *136*(1–2), 725–740. https://doi.org/10.1130/B36791.1

Teyssier, C., Ferré, E. C., Whitney, D. L., Norlander, B., Vanderhaeghe, O., & Parkinson, D. (2005). Flow of partially molten crust and origin of detachments during collapse of the Cordilleran Orogen. *Geological Society, London, Special Publications*, *245*(1), 39–64. https://doi.org/10.1144/GSL.SP.2005.245.01.03

Thoresen, H. E., Cassel, E. J., Smith, M. E., Stockli, D. F., & Jicha, B. R. (2024). Stratigraphic and geochronologic investigation of the Muddy Creek Basin: Implications for the Eocene tectonic evolution of southwest Montana, USA. *Geological Society of America Bulletin*, *136*(9–10), 3619–3633. https://doi.org/10.1130/B37268.1

Tirel, C., Brun, J., & Burov, E. (2008). Dynamics and structural development of metamorphic core complexes. *Journal of Geophysical Research*, *113*(B4), 2005JB003694. https://doi.org/10.1029/2005JB003694

Turner, S. J., Langmuir, C. H., Katz, R. F., Dungan, M. A., & Escrig, S. (2016). Parental arc magma compositions dominantly controlled by mantle-wedge thermal structure. *Nature Geoscience*, *9*(10), 772–776. https://doi.org/10.1038/ngeo2788

Valencia-Moreno, M., López-Martínez, M., Orozco-Esquivel, T., Ferrari, L., Calmus, T., Noury, M., & Mendívil-Quijada, H. (2021). The Cretaceous-Eocene Mexican Magmatic Arc: Conceptual framework from geochemical and geochronological data of plutonic rocks. *Earth-Science Reviews*, *220*, 103721. https://doi.org/10.1016/j.earscirev.2021.103721

Vejmelek, L., & Smithson, S. B. (1995). Seismic reflection profiling in the Boulder batholith, Montana. *Geology*, *23*(9), 811–814. https://doi.org/10.1130/0091-7613(1995)023<0811:SRPITB>2.3.CO;2

Walker, J. D., Bowers, T. D., Black, R. A., Glazner, A. F., Lang Farmer, G., & Carlson, R. W. (2006). A geochemical database for western North American volcanic and intrusive rocks (NAVDAT). In A. K. Sinha (Ed.), *Geoinformatics: Data to knowledge* (pp. 61–71). Geological Society of America. https://doi.org/10.1130/2006.2397(05)

Weil, A. B., & Yonkee, A. (2023). The Laramide orogeny: Current understanding of the structural style, timing, and spatial distribution of the classic foreland thick-skinned tectonic system. In S. J. Whitmeyer, M. L. Williams, D. A. Kellett, & B. Tikoff (Eds.), *Laurentia: Turning points in the evolution of a continent* (pp. 707–771). Geological Society of America. https://doi.org/10.1130/2022.1220(33)

Wells, M. L., Hoisch, T. D., Cruz-Uribe, A. M., & Vervoort, J. D. (2012). Geodynamics of synconvergent extension and tectonic mode switching: Constraints from the Sevier-Laramide orogen. *Tectonics*, *31*(1), 2011TC002913. https://doi.org/10.1029/2011TC002913

Wells, M. L., Dallmeyer, R. D., & Allmendinger, R. W. (1990). Late Cretaceous extension in the hinterland of the Sevier thrust belt, northwestern Utah and southern Idaho. *Geology*, *18*(10), 929. https://doi.org/10.1130/0091-7613(1990)018<0929:LCEITH>2.3.CO;2

Wells, M. L., & Hoisch, T. D. (2008). The role of mantle delamination in widespread Late Cretaceous extension and magmatism in the Cordilleran orogen, western United States. *Geological Society of America Bulletin*, *120*(5–6), 515–530. https://doi.org/10.1130/B26006.1

Wernicke, B. (1992). Cenozoic extensional tectonics of the U.S. Cordillera. In B. C. Burchfiel, P. W. Lipman, & M. L. Zoback (Eds.), *The Cordilleran Orogen* (Vol. G-3, pp. 553–581). Geological Society of America. https://doi.org/10.1130/DNAG-GNA-G3.553

Wernicke, B. P., England, P. C., Sonder, L. J., & Christiansen, R. L. (1987). Tectonomagmatic evolution of Cenozoic extension in the North American Cordillera. *Geological Society, London, Special Publications*, *28*(1), 203–221. https://doi.org/10.1144/GSL.SP.1987.028.01.15

Whitney, D. L., Teyssier, C., Rey, P., & Buck, W. R. (2013). Continental and oceanic core complexes. *Geological Society of America Bulletin*, *125*(3–4), 273–298. https://doi.org/10.1130/B30754.1

Wijns, C., Weinberg, R., Gessner, K., & Moresi, L. (2005). Mode of crustal extension determined by rheological layering. *Earth and Planetary Science Letters*, *236*(1–2), 120–134. https://doi.org/10.1016/j.epsl.2005.05.030

Wolfe, J. A., Forest, C. E., & Molnar, P. (1998). Paleobotanical evidence of Eocene and Oligocene paleoaltitudes in midlatitude western North America. *Geological Society of America Bulletin*, *110*(5), 664–678. https://doi.org/10.1130/0016-7606(1998)110<0664:PEOEAO>2.3.CO;2

Yonkee, W. A., & Weil, A. B. (2015). Tectonic evolution of the Sevier and Laramide belts within the North American Cordillera orogenic system. *Earth-Science Reviews*, *150*, 531–593. https://doi.org/10.1016/j.earscirev.2015.08.001

Zuza, A. V., & Cao, W. (2023). Metamorphic core complex dichotomy in the North American Cordillera explained by buoyant upwelling in variably thick crust. *Geological Society of America Today*, *33*(3–4), 4–11. https://doi.org/10.1130/GSATG548A.1

Zuza, A. V., Cao, W., Levy, D. A., DesOrmeau, J. W., Odlum, M. L., & Siciliano, A. A. (2024). Kinematic vorticity of shear zones that accommodate vertical crustal advection: Implications for metamorphic core complexes and pluton emplacement. *Earth and Planetary Science Letters*, *646*, 118964. https://doi.org/10.1016/j.epsl.2024.118964
Zuza, A. V., Jepson, G., & Cao, W. (2024). Reassessing metamorphic core complexes in the North American Cordillera. *Earth-Science Reviews*, *260*, 104987. https://doi.org/10.1016/j.earscirev.2024.104987